RESEARCH ARTICLE

Plio-Pleistocene evolution of water mass exchange and erosional input at the Atlantic-Arctic gateway

Claudia Teschner[1,2], Martin Frank[1], Brian A. Haley[3], and Jochen Knies[4,5]

[1]GEOMAR, Helmholtz Centre for Ocean Research Kiel, Kiel, Germany, [2]Now at Department of Earth and Environmental Sciences, Section for Mineralogy, Petrology, and Geochemistry, LMU, Ludwig-Maximilians-Universität München, Munich, Germany, [3]CEOAS, College of Earth, Oceanic, and Atmospheric Sciences, Oregon State University, Corvallis, Oregon, USA, [4]Geological Survey of Norway, Trondheim, Norway, [5]CAGE-Centre for Arctic Gas Hydrate, Environment and Climate, Department of Geology, University of Tromsø, Tromsø, Norway

Abstract Water mass exchange between the Arctic Ocean and the Norwegian-Greenland Seas has played an important role for the Atlantic thermohaline circulation and Northern Hemisphere climate. We reconstruct past water mass mixing and erosional inputs from the radiogenic isotope compositions of neodymium (Nd), lead (Pb), and strontium (Sr) at Ocean Drilling Program site 911 (leg 151) from 906 m water depth on Yermak Plateau in the Fram Strait over the past 5.2 Myr. The isotopic compositions of past bottom waters were extracted from authigenic oxyhydroxide coatings of the bulk sediments. Neodymium isotope signatures obtained from surface sediments agree well with present-day deepwater ε_{Nd} signature of -11.0 ± 0.2. Prior to 2.7 Ma the Nd and Pb isotope compositions of the bottom waters only show small variations indicative of a consistent influence of Atlantic waters. Since the major intensification of the Northern Hemisphere Glaciation at 2.7 Ma the seawater Nd isotope composition has varied more pronouncedly due to changes in weathering inputs related to the waxing and waning of the ice sheets on Svalbard, the Barents Sea, and the Eurasian shelf, due to changes in water mass exchange and due to the increasing supply of ice-rafted debris (IRD) originating from the Arctic Ocean. The seawater Pb isotope record also exhibits a higher short-term variability after 2.7 Ma, but there is also a trend toward more radiogenic values, which reflects a combination of changes in input sources and enhanced incongruent weathering inputs of Pb released from freshly eroded old continental rocks.

1. Introduction

The Arctic Ocean and the Norwegian-Greenland Seas (NGS) have played an important role in determining the strength of thermohaline circulation, as well as in controlling Northern Hemisphere climate evolution. Outside the Labrador Sea, the NGS are the most important areas for the formation of cold and saline deep waters contributing to the export of North Atlantic Deep Water (NADW). The NADW is responsible for the ventilation of the present-day deep Atlantic Ocean as part of the Atlantic meridional overturning circulation (AMOC) [*Broecker et al.*, 1985; *Rahmstorf*, 2002; *Kuhlbrodt et al.*, 2007]. The AMOC is of primary importance for the modern climate system because it influences the supply of heat to the high latitudes and thus regulates the extent of the sea ice in the NGS. Many studies have shown that the AMOC underwent drastic changes in the past [*Imbrie et al.*, 1993; *de Menocal et al.*, 1992; *Boyle*, 1988; *Böhm et al.*, 2015]. Severe reductions or even shutdowns of the AMOC during distinct cold periods in the past have been inferred as a consequence of diminished surface water salinity in the NGS caused either by enhanced supply of low-salinity surface waters from the Arctic Ocean or by freshwater input originating from glacial meltwaters [e.g., *Knies et al.*, 2007; *Brinkhuis et al.*, 2006; *Peltier et al.*, 2006; *Clark et al.*, 2002; *Ganopolski and Rahmstorf*, 2001]. Similar freshwater-triggered "slowdowns" of the AMOC may occur in the near future due to accelerated melting of the ice sheets in response to anthropogenic forcing [*Peterson et al.*, 2006], although the extent of this effect may not be as significant as previously thought [*Böhm et al.*, 2015]. The goal of our study is to provide new insights into the evolution of the high-latitude deep ocean circulation and of Arctic-Atlantic water mass exchange, which has influenced the formation of deep waters in the NGS.

1.1. Plio-Pleistocene Evolution of High Northern Latitude Climate and Ocean Circulation

The onset and major intensification of the Northern Hemisphere Glaciation (iNHG) was one of the most important shifts in global climate of the Cenozoic [*Zachos et al.*, 2001]. Despite the first occurrence of

ice-rafted debris (IRD) in central Arctic sediments as early as 45 Ma [*Moran et al.*, 2006] and in the NGS between 38 and 30 Ma [*Eldrett et al.*, 2007], clear evidence for a first significant continental glaciation of the Northern Hemisphere was only found during the late Miocene as the development of an ice sheet on southern Greenland [*Wolf-Welling et al.*, 1995; *Wolf and Thiede*, 1991; *Jansen and Sjøholm*, 1991]. At 3.3 Ma distinct IRD peaks are documented for the Nordic Seas indicating a pronounced glacial expansion in the Northern Hemisphere with the Greenland ice sheet as the most important source of IRD [*Jansen et al.*, 2000; *Kleiven et al.*, 2002; *Knies et al.*, 2014a]. During this period reduced sea surface temperatures in the North Atlantic Ocean of about 2–3°C are documented, linked to a reduced heat transport toward the high northern latitudes [*De Schepper et al.*, 2013]. The Pliocene climate optimum from 3.29 to 2.97 Ma was marked by increased global annual mean temperatures [*Dowsett et al.*, 2012, 2013] indicating warmer and relative stable climatic conditions. Subsequently, a major change of the climatic conditions prevailing in the Norwegian Sea has been observed from a marked increase in the supply and deposition of IRD in the NGS beginning at isotope stage G6 (2.72 Ma) [e.g., *Knies et al.*, 2014a, 2014b; *Kleiven et al.*, 2002; *Jansen et al.*, 2000; *Fronval and Jansen*, 1996]. Overall, the intensification of the Northern Hemisphere Glaciation has been described as a gradual process between 3.6 and 2.4 Ma, as deduced from marine δ^{18}O records [*Mudelsee and Raymo*, 2005], with three pronounced IRD peaks at 3.6 Ma, 3.3 Ma, and 2.7 Ma on the Yermak Plateau [*Knies et al.*, 2014a].

There are different hypotheses explaining the intensification of the NHG including orbital forcing [*Maslin et al.*, 1996; *Huybers and Molnar*, 2007], closure of the Indonesian gateway [*Cane and Molnar*, 2001; *Karas et al.*, 2009], final closure of the Isthmus of Panama [*Sarnthein et al.*, 2009, and references therein], and a decline in atmospheric CO_2 [*Lunt et al.*, 2008]. A strong east-west temperature gradient and a modern-like circulation in the Nordic Seas intensifying the NADW formation already developed at 4.5 Ma as consequence of the evolution of the connection between the North Pacific and Arctic Ocean [*De Schepper et al.*, 2015]. Around 2.7 Ma marked changes in planktonic and benthic δ^{18}O records [*Driscoll and Haug*, 1998; *Haug and Tiedemann*, 1998; *Bartoli et al.*, 2005; *Mudelsee and Raymo*, 2005; *Lisiecki and Raymo*, 2005], and of the radiogenic isotope composition of deep waters in the western North Atlantic [*Burton et al.*, 1999; *Frank et al.*, 1999; *Reynolds et al.*, 1999; *Frank*, 2002] documented a temperature drop, enhanced ice sheet buildup and related erosional inputs in the high northern latitudes, as well as a significant change of the Atlantic Ocean circulation.

While the water mass exchange between the Arctic Ocean and the NGS has clearly been critical for the climate system, its long-term variability has so far remained largely unconstrained. The latter is mainly a consequence of the almost complete absence of foraminifera in Arctic Ocean sediments. In the present study, we thus apply radiogenic Nd and Pb isotopes extracted from Yermak Plateau sediments as proxies for past water mass composition and mixing between the Arctic and Atlantic Oceans, as well as for changes in erosional inputs and the continental weathering regime during the past 5.2 Myr.

1.2. Tracing Water Masses with Radiogenic Nd and Pb Isotopes

The radiogenic isotope composition of Nd in seawater reveals changes in water mass mixing and circulation patterns due to its quasi-conservative behavior [*Frank*, 2002; *Goldstein et al.*, 2003] and average oceanic residence time of 360–2000 years [*Tachikawa et al.*, 1999; *Arsouze et al.*, 2009; *Rempfer et al.*, 2011] similar to the global ocean mixing time of about 1500 years [*Broecker and Peng*, 1982]. In addition, the different isotopic compositions of detrital particles provide information about the source and pathways of the sediments [e.g., *Hemming*, 2004; *Haley et al.*, 2008b; *Maccali et al.*, 2012]. The neodymium isotopic composition is expressed as $\varepsilon_{\text{Nd}} = [(^{143}\text{Nd}/^{144}\text{Nd})_{\text{sample}}/(^{143}\text{Nd}/^{144}\text{Nd})_{\text{CHUR}} - 1] \times 10,000$, wherein a $^{143}\text{Nd}/^{144}\text{Nd} = 0.512638$ for present-day Chondritic Uniform Reservoir (CHUR) is applied [*Jacobsen and Wasserburg*, 1980]. Unlike other isotope systems, such as those of oxygen or carbon, Nd isotope ratios are not influenced by isotope fractionation caused by biological and other low-temperature processes. The Nd isotope composition of past seawater can be extracted from different sedimentary archives. Besides fish teeth [e.g., *Martin et al.*, 2010, 2012], the Nd isotope composition of early diagenetic ferromanganese coatings of marine sediments has successfully been used to reconstruct bottom water Nd isotope compositions at different locations in the Southern Ocean [*Rutberg et al.*, 2000; *Piotrowski et al.*, 2004, 2005; *Molina-Kescher et al.*, 2014], the Indian Ocean [*Piotrowski et al.*, 2009; *Wilson et al.*, 2012], the North Atlantic Ocean [*Gutjahr et al.*, 2008; *Gutjahr and Lippold*, 2011; *Werner et al.*, 2014; *Khélifi and Frank*, 2014; *Khélifi et al.*, 2014; *Böhm et al.*, 2015], and the Arctic Ocean [*Haley et al.*, 2008a; *Chen et al.*, 2012; *Haley and Polyak*, 2013]. In addition, planktonic foraminifera
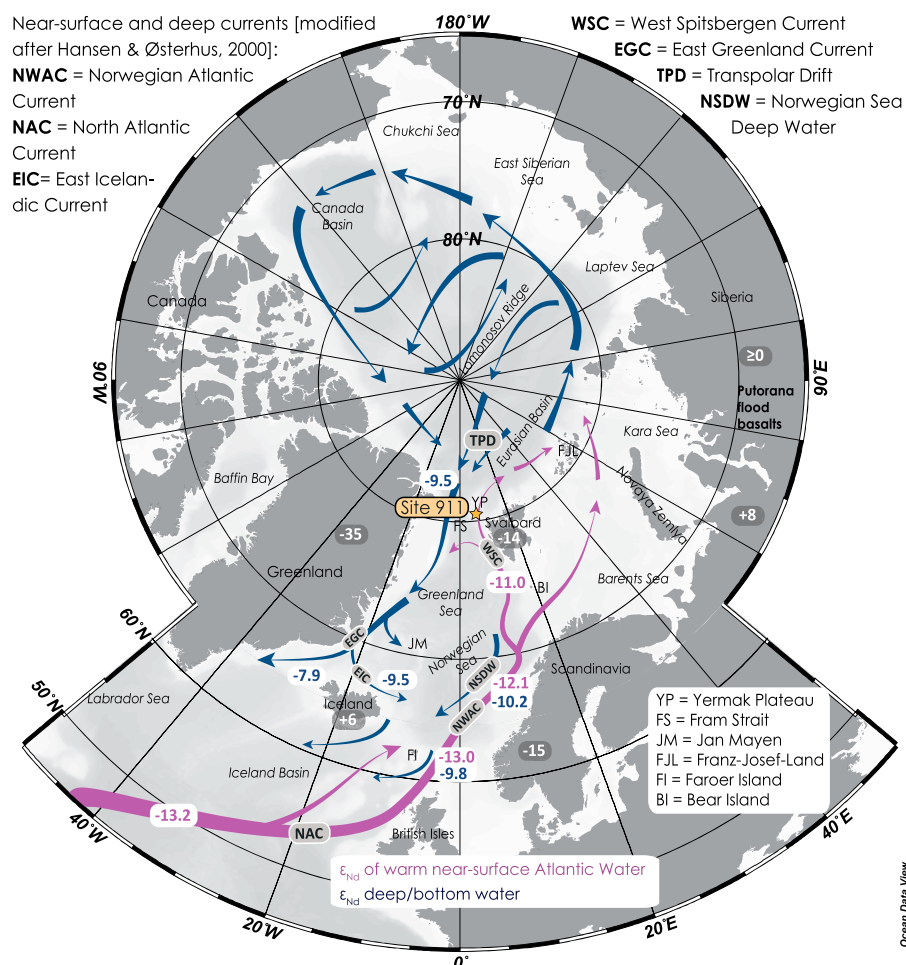
Figure 1. Map of the North Atlantic and Norwegian-Greenland Seas (Nordic Seas) and study site 911 together with schematic flow paths of the main water masses [*Hansen and Østerhus*, 2000] and their present-day ε_{Nd} signatures. Purple arrows mark the warm inflowing Atlantic water; dark blue arrows represent the cold deep and surface water masses flowing out of the Arctic Ocean, as well as the deep waters in the Norwegian-Greenland Sea [*Lacan and Jeandel*, 2004a, 2004b; *Andersson et al.*, 2008]. White numbers mark the average ε_{Nd} values of the bedrocks of Svalbard [*Tütken et al.*, 2002], the Norwegian Caledonian Margin and Iceland [*Lacan and Jeandel*, 2004b, and references therein], the Putorana basalts in Russia [*Sharma et al.*, 1992], and Greenland [*Lacan and Jeandel*, 2004a, and references therein].

and their authigenic ferromanganese coatings were applied for the reliable reconstruction of the Nd isotope composition of bottom waters [*Roberts et al.*, 2010, 2012; *Piotrowski et al.*, 2012; *Kraft et al.*, 2013; *Tachikawa et al.*, 2014].

Lead (Pb) has a much shorter residence time of only about 50 years in the Atlantic Ocean [*Schaule and Patterson*, 1981; *Erel et al.*, 1994] and therefore provides a more localized dissolved seawater signal mainly reflecting the erosional input from nearby continental rocks and exchange processes with the continental margins [*Frank*, 2002; *Gutjahr et al.*, 2009; *Crocket et al.*, 2013; *Wilson et al.*, 2015]. In addition, Pb experiences pronounced incongruent weathering as a consequence of the α-recoil effect causing fractionation of the Pb isotopes during formation of the chemical weathering solutions prior to transport to the oceans. Specifically, the radioactive decay of the U-series isotopes causes damages of the crystal structure of the minerals, which leads to preferential mobilization of the radiogenic Pb isotopes (^{206}Pb, ^{207}Pb, and ^{208}Pb) over primordial ^{204}Pb, in particular from freshly exposed old granitic rocks [*Erel et al.*, 1994; *von Blanckenburg and Nägler*, 2001].

Important sources for both dissolved Nd and Pb in seawater are eolian and riverine inputs [e.g., *Frank*, 2002, and references therein], as well as boundary exchange with the continental shelf sediments, during which the Nd and Pb isotopic compositions of the bottom waters near the continental margins can be significantly

modified [e.g., *Jeandel et al.*, 1998; *Lacan and Jeandel*, 2005a; *Wilson et al.*, 2013, 2015]. It is still not well understood, however, which exact mechanisms control such changes of the Nd isotopic composition of the bottom waters and which sediment phases are involved. Nonetheless, the effects of boundary exchange have been clearly observed along different continental margins in the subpolar regions including the Nordic Seas [*Lacan and Jeandel*, 2004a, 2005a], and modeling results confirmed the importance of this input mechanism [*Arsouze et al.*, 2009; *Rempfer et al.*, 2011]. Due to the large shelf areas of the Arctic Ocean boundary exchange might be expected to be significant, although the water column data available so far do not provide clear evidence for this process [*Andersson et al.*, 2008; *Porcelli et al.*, 2009]. In the case of the Mediterranean Arctic Ocean basin, both the riverine Nd input in particulate [*Eisenhauer et al.*, 1999; *Haley et al.*, 2008a] and in dissolved form [*Andersson et al.*, 2008; *Porcelli et al.*, 2009] are important contributors. In addition, ice sheet and sea ice transport of particulates and their partial dissolution in the water column are expected to have played a relevant role for the supply of dissolved Nd into the Arctic Ocean. These input and exchange mechanisms control the isotope composition of the water masses in the Nordic Seas and the Fram Strait leading to distinct ε_{Nd} values.

1.3. Hydrographic Setting

The Fram Strait is the only deepwater connection (~2600 m mean water depth) between the Arctic and Atlantic Oceans. The water masses in the Fram Strait and on Yermak Plateau (Figure 1) are dominated by inflowing Atlantic water [*Rudels et al.*, 2000, 2005], which enters the Norwegian Sea as part of the relatively warm and saline near-surface North Atlantic Current (NAC). The NAC crosses the Iceland-Faroe Ridge and Faroe-Shetland Channel to flow northward, where it encounters the colder, less saline waters of the East Iceland Current. The warm NAC is characterized by ε_{Nd} values of -13.2 to -13.0 at its areas of origin in the North Atlantic ($T > 5°C$; $S > 35.0$) [*Piepgras and Wasserburg*, 1987; *Lacan and Jeandel*, 2004b, 2005b]. The warm Atlantic sourced water remains traceable as the Norwegian Atlantic Current (NWAC) at the western shelf of Norway [*Hansen and Østerhus*, 2000] (Figure 1). Southwest of Svalbard at 600 m water depth the inflowing Atlantic water has an ε_{Nd} value of -11.0 ± 0.2, which is significantly more radiogenic than the core of the inflowing Atlantic water detected at water depths between 200 and 400 m further south at 60°N, where the ε_{Nd} signature is -13.0 [*Lacan and Jeandel*, 2004b]. The more radiogenic values found off Svalbard are caused by mixing with Norwegian Sea Deep Water ($\varepsilon_{Nd} = -10.2 \pm 0.2$) [*Lacan and Jeandel*, 2004b]. On the Yermak Plateau the warmer subsurface Atlantic-sourced water [*Rudels et al.*, 2000, 2005] is the dominant water mass occupying depths between 250 and 1000 m [*Karcher and Oberhuber*, 2002]. The NWAC flows into the Arctic Ocean via its main branch through Fram Strait [*Rudels et al.*, 2000; *Karcher and Oberhuber*, 2002], where it cools and continues northward into the Arctic Ocean as the subsurface West Spitsbergen Current. The water masses forming the Arctic Ocean outflow pass through the western Fram Strait and flow south into Denmark Strait as the East Greenland Current (Figure 1), which transports sea ice and cold, low-salinity Arctic surface waters, as well as denser water masses from the Arctic basin into the North Atlantic Ocean [*Rudels et al.*, 2005]. The deep waters and the polar mixed layer flowing out the Arctic Ocean appear to have a somewhat more radiogenic Nd isotope composition in the western part of the Fram Strait (between -9.5 and -9.8 ± 0.4) compared to the eastern inflow branches [*Andersson et al.*, 2008]. Further south in the Denmark Strait the Nd isotopic compositions range from -10.8 ± 0.2 for the surface waters to -7.9 ± 0.6 for the intermediate water at ~500 m depth [*Lacan and Jeandel*, 2004a, 2004b].

Ocean Drilling Program (ODP) site 911 on Yermak Plateau (ODP leg 151 [*Myhre et al.*, 1995]) is located within the influence of the warm modified Atlantic waters from the south (80°28.466′N, 08°13.640′E; 906 m water depth). While the deep and intermediate waters are dominated by the Atlantic export into the Arctic Ocean, the Transpolar Drift (TPD) controls the surface water flow of the eastern Fram Strait at the location of site 911, as well as of the Barents Sea and Svalbard shelves [*Gordienko and Laktionov*, 1969]. Icebergs and sea ice with incorporated sediments from the Siberian shelf (Kara/Laptev Sea) are exported toward Fram Strait, where they melt when the TPD encounters the warmer Atlantic water resulting in the release of their entrained IRD [*Pfirman et al.*, 1997].

1.4. Changes in Arctic Circulation Over the Past 5.2 Myr

To date there have only been few studies reconstructing past water mass mixing and sediment transport in the Arctic Ocean and the Fram Strait on the basis of radiogenic Nd and Pb isotopes. *Winter et al.* [1997] reconstructed changes of sediment sources, weathering inputs, and deepwater masses using radiogenic isotope compositions of diagenetic micronodules, foraminifera, and bulk sediment extracted from deep-sea

sediments in the central Arctic Ocean (Alpha Ridge) spanning approximately the past 6 Myr. In that study a significant increase in $^{87}Sr/^{86}Sr$ and $^{206}Pb/^{204}Pb$ ratios and a decrease in ε_{Nd} signatures of the silicate fraction since ~1.7 Ma were observed. This was interpreted in terms of a change in the main sediment transport mechanism from deposition by sea ice to glacial ice-rafted detritus (IRD), as well as a change in sediment provenance to source areas in northern Canada and Queen Elizabeth Island. Recently, *Dausmann et al.* [2015] confirmed and extended these findings based on new time series data obtained from well-dated ferromanganese crusts from the Northwind Ridge in the Canada basin and showed that increased weathering inputs from these source areas forced by the onset of NHG already started approximately 4 Myr ago.

Haley et al. [2008a, 2008b] and *Chen et al.* [2012] reconstructed the dissolved Nd, Pb, and Hf isotope evolution of Arctic Intermediate Water from ferromanganese coatings of bulk sediments from the Lomonosov Ridge following the modified methods of *Bayon et al.* [2002] and *Gutjahr et al.* [2007] over the past 15 Myr. These authors reported a major switch from long-term stable hydrographic conditions prior to the onset of the NHG to a pronounced variability of Atlantic inflow, as well as of brine formation on the Siberian shelf on glacial/interglacial time scales thereafter. Brine rejection and formation of saline and dense water masses occur during sea ice formation on shallow shelves surrounding the Arctic basin [e.g., *Aagaard et al.*, 1985], and near the Kara Sea these brines have been suggested to incorporate the highly radiogenic Nd isotope signature of the shelf sediments largely originating from the Putorana basalts during maximum ice sheet extent [*Haley et al.*, 2008a]. A recent study focused on the evolution of water mass exchange and sediment transport based on variations of Pb isotope signatures of the leached and detrital fractions along a transect across Fram Strait at 79°N from the Last Glacial Maximum to the present [*Maccali et al.*, 2012]. In that study, the Canadian and Siberian shelves, as well as Greenland, were found to have been the main sources of detrital material exported through Fram Strait via sea ice and icebergs, which also influenced the leached Pb isotope composition of past bottom waters. More recently, *Werner et al.* [2014] applied Nd isotopes for the reconstruction of changes in source and mixing of bottom water masses at the West Spitsbergen continental margin over the past 8500 years. Their data indicate a reduced inflow of Atlantic water masses and a shift of the marginal ice zone during the late Holocene.

Here we present the first reconstruction of water mass exchange as well as erosional inputs and sediment transport across the Yermak Plateau in the Fram Strait covering the past 5.2 Myr with a particular focus on the onset of Northern Hemisphere Glaciation. We apply radiogenic isotope signatures of past seawater extracted from early diagenetic ferromanganese coatings, as well as of the detrital fraction itself.

2. Material and Methods

Sediments of ODP site 911 (leg 151) from a water depth of 906 m (80°28.466′N, 08°13.640′E) have been analyzed in this study. The stratigraphy and composition of the sediments of this core have been subject to several previous studies [*Knies et al.*, 2002, 2009], and we apply the age model of *Knies et al.* [2009] for the interval <2.7 Ma, which is based on magnetostratigraphy and calcareous nanofossils. For the core sections prior to 2.7 Ma, we base our study on the new stratigraphic framework of site 911 recently established by *Knies et al.* [2014a, 2014b] including the seismostratigraphic data of *Mattingsdal et al.* [2014] and biostratigraphic results of *Grøsfjeld et al.* [2014]. In total, 12 tie points are the basis of the age model (Table S2 in the supporting information), and linear interpolation of the sedimentation rates between them was applied to derive the age model.

Radiogenic isotopes of Nd and Pb are used for paleoenvironmental reconstruction. We applied the method of *Gutjahr et al.* [2007] to extract the Nd, Pb, and Sr isotope compositions of past bottom water incorporated into authigenic ferromanganese oxyhydroxide coatings on the sediment particles. Similar to previous studies of central Arctic sediments [*Haley et al.*, 2008a, 2008b; *Chen et al.*, 2012] and given the carbonate content of the sediments at site 911 only reaching between 1% and 6% [*Myhre et al.*, 1995], a carbonate removal step was not included in the leach procedure. The procedure thus directly started with extracting the past seawater signal contained in the diagenetic coatings from ~2 g of sample material with a 0.05 M hydroxylamine hydrochloride/15% acetic acid solution (HH leach), buffered to a pH of ~3.5 to 4.0, without rinsing before the HH leach. Furthermore, the $MgCl_2$ step to remove metals adsorbed to the particle surfaces [*Gutjahr et al.*, 2007] was also omitted because *Haley et al.* [2008a, 2008b] found that there was no measureable difference in the isotopic compositions of Nd, Pb, and Sr extracted from Arctic Ocean sediments with or

without this step. The radiogenic $^{87}Sr/^{86}Sr$ ratio in the solutions containing the seawater-derived extracted metals was monitored to identify detrital contamination by major deviations from the expected seawater signature of the past 5.2 Myr, while acknowledging that this does not provide an unambiguous measure of such contamination for the Nd and Pb isotope data [*Gutjahr et al.*, 2007].

After separation of the leach solution by centrifugation, the remaining sediment was allowed to react with additional hydroxylamine solution for at least 12 more hours to guarantee complete removal of any authigenic coatings left on the particles following *Haley et al.* [2008b]. Afterward, the detrital fraction was rinsed with deionized water 3 times, dried, and ground to prepare for the total digestion of the detrital fraction. Fifty milligrams of the ground sediment was weighed and dissolved in a mixture of concentrated HNO_3 + HF at 180°C over 3 days. The samples were evaporated to dryness and treated with a mixture of HNO_3 + $HClO_4$ at 190°C to destroy remaining organic material prior to the ion chromatographic separation and purification steps.

In a first step Pb was separated from the solutions on anion exchange columns containing 50 μL of AG1-X8 resin (mesh 100–200) following the method of *Lugmair and Galer* [1992]. The rare earth elements (REEs) and the Sr in the remaining solution were separated using cation exchange columns filled with 0.8 mL AG50W-X12 resin (mesh 200–400) [*Barrat et al.*, 1996]. The Sr cut was further purified on columns with 50 μL Sr-Spec resin (mesh 50–100) following the method of *Horwitz et al.* [1992] and *Bayon et al.* [2002]. Using columns with 2 mL Ln-Spec resin (50–100 mesh) the Nd was separated from the other REEs [*Le Fèvre and Pin*, 2005].

All measurements were carried out on a *Nu Plasma* Multi Collector ICP-MS at GEOMAR, Kiel. Mass bias corrections were carried out using a value of 0.7219 for the $^{146}Nd/^{144}Nd$, and instrument bias was normalized to the accepted $^{143}Nd/^{144}Nd$ value of the JNdi-1 standard of 0.512115 [*Tanaka et al.*, 2000]. Repeated measurements of this standard yielded a long-term reproducibility for the JNdi-1 standard solution of ±0.3 ε_{Nd} (2σ; $n = 120$) over a period of 16 months. The procedural blanks for Nd were ≤80 pg. Similarly, $^{86}Sr/^{88}Sr = 0.1194$ was applied for mass bias correction of the Sr isotope measurements [*Steiger and Jäger*, 1977] while also correcting for interferences of ^{86}Kr and ^{87}Rb. The Sr isotope results were normalized for instrument bias using to $^{87}Sr/^{86}Sr = 0.710245$ of the National Institute of Standards and Technology (NIST) National Bureau of Standards (NBS)987 standard, which was also used to derive the long-term reproducibility of the radiogenic Sr isotope measurements of ±0.000032 (2σ; $n = 70$) over 1 year. The procedural blanks for Sr were below 2 ng. The Pb isotope ratios were analyzed following the standard bracketing method of *Albarède et al.* [2004], without the addition of thallium, and all measured data were normalized for instrument bias using the accepted values for NIST NBS981 of $^{206}Pb/^{204}Pb = 16.9405$, $^{207}Pb/^{204}Pb = 15.4963$, and $^{208}Pb/^{204}Pb = 36.7219$ [*Abouchami et al.*, 1999]. The long-term reproducibility (2σ; $n = 88$) over 1 year for this standard was ±0.008 for $^{206}Pb/^{204}Pb$, ±0.009 for $^{207}Pb/^{204}Pb$, ±0.033 for $^{208}Pb/^{204}Pb$, ±0.0009 for $^{208}Pb/^{206}Pb$, and ±0.0002 for $^{207}Pb/^{206}Pb$. The procedural blanks for all Pb isotope measurements were ≤1.45 ng.

3. Results

3.1. Neodymium and Strontium Isotopic Signatures of Leachates and the Detrital Sediment Fraction

The ε_{Nd} signatures of the leached coatings vary between −6.9 and −12.1 (Figure 2). The core top value (0–3 cm) of −11.0 falls in the range of the values for present-day deep water at this site [*Lacan and Jeandel*, 2004b; *Andersson et al.*, 2008] (Figure 3). The different resolution of the ε_{Nd} records before and after 2.7 Ma is due to the focus on the evolution of the water mass exchange after the intensification of the Northern Hemisphere Glaciation (iNHG). Prior to the iNHG at 2.7 Ma the deepwater ε_{Nd} on the Yermak Plateau ranged from −8.5 to −11.5 (with a mean ε_{Nd} of −10.4 and a range of 3 ε_{Nd} units), whereas after 2.7 Ma the amplitude of the ε_{Nd} variability almost doubled to 5.2 ε_{Nd} units and varied between −6.9 and −12.1. While the unradiogenic baseline of the ε_{Nd} data remained close to −11.5, the radiogenic peaks were more pronounced after the iNHG (Figure 2). No statistically significant long-term trend ($r^2 = 9 \times 10^{-6}$) of the deepwater Nd isotope composition is observed for the past 5.2 Myr at site 911.

The Nd isotopic compositions of the leachates and the detrital material show a close coupling (Figure S1 in the supporting information), whereby the detrital fraction of the Fram Strait sediments has overall less radiogenic Nd isotope compositions (between −8.4 and −12.9) than the corresponding authigenic coatings (Figure 2). However, similar to the leachate compositions the amplitude of the detrital Nd isotope variability more than
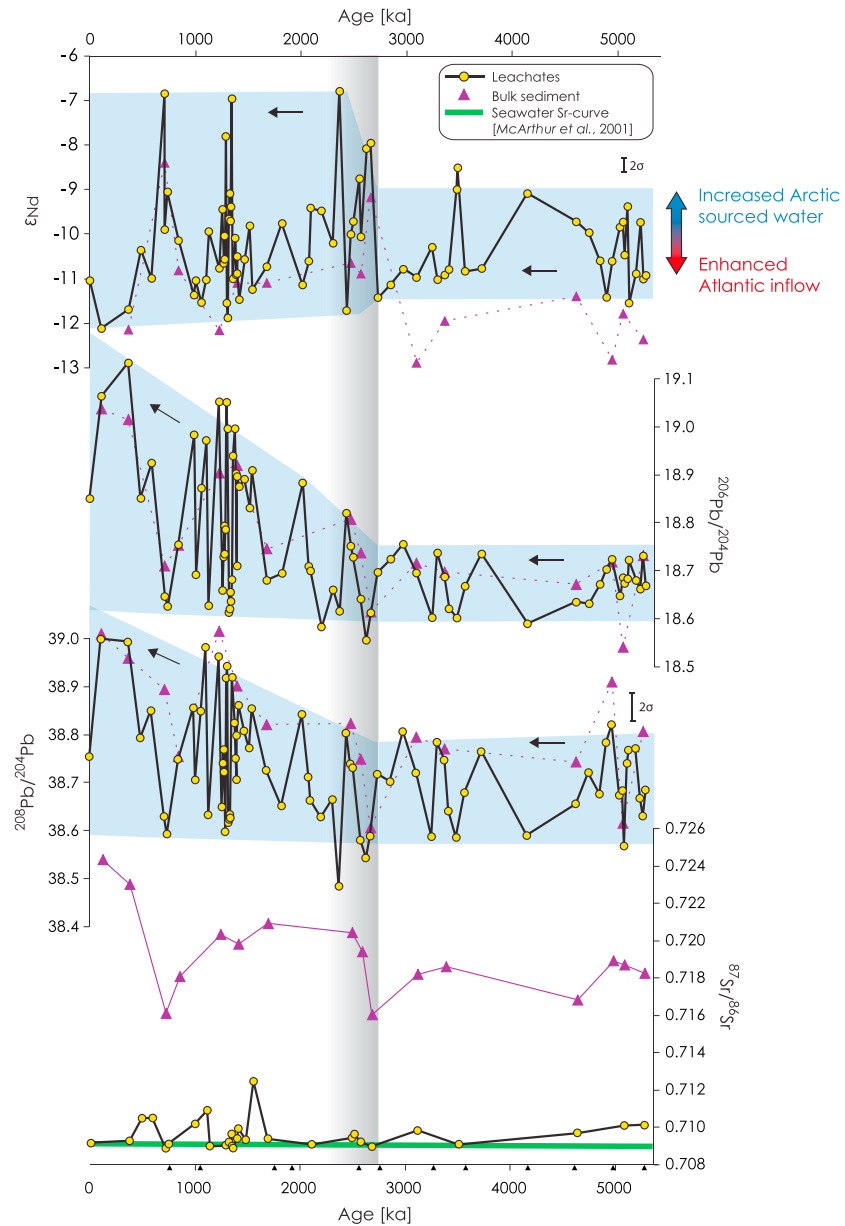
Figure 2. Evolution of the radiogenic Nd, Pb, and Sr isotope compositions of reductive leachates (yellow dots) and of bulk sediment (purple triangles) of site 911 for the past 5.2 Myr. The 2σ errors for ^{206}Pb/^{204}Pb and Sr isotope measurements are smaller than symbol size. The 2σ error for ε_{Nd} and ^{208}Pb/^{204}Pb is given as black bar. The green line in the bottom plot denotes the Sr isotope evolution of global seawater [*McArthur et al.*, 2001] over the past 5.2 Myr. The area shaded in blue highlight the amplitude and trends of the Nd and Pb isotope evolution. The shaded grey bar marks the major intensification of the Northern Hemisphere Glaciation.

doubled from 1.4 ε_{Nd} units prior to 2.7 Ma to 3.8 ε_{Nd} units thereafter. The average detrital ε_{Nd} and ^{87}Sr/^{86}Sr values of −11.5 and of 0.71867, respectively, are consistent with previous analyses of late Quaternary sediments from the Yermak Plateau [*Tütken et al.*, 2002].

3.2. Lead Isotope Signatures of Leachates and the Detrital Sediment Fraction

The Pb isotope evolution and increasing amplitude of variability at site 911 resembled that of the Nd isotopes, but in contrast to the Nd isotope record and despite the large-amplitude variability there has been an overall trend toward more radiogenic Pb values after the onset of the NHG ($r^2 = 0.213$). The ^{206}Pb/^{204}Pb
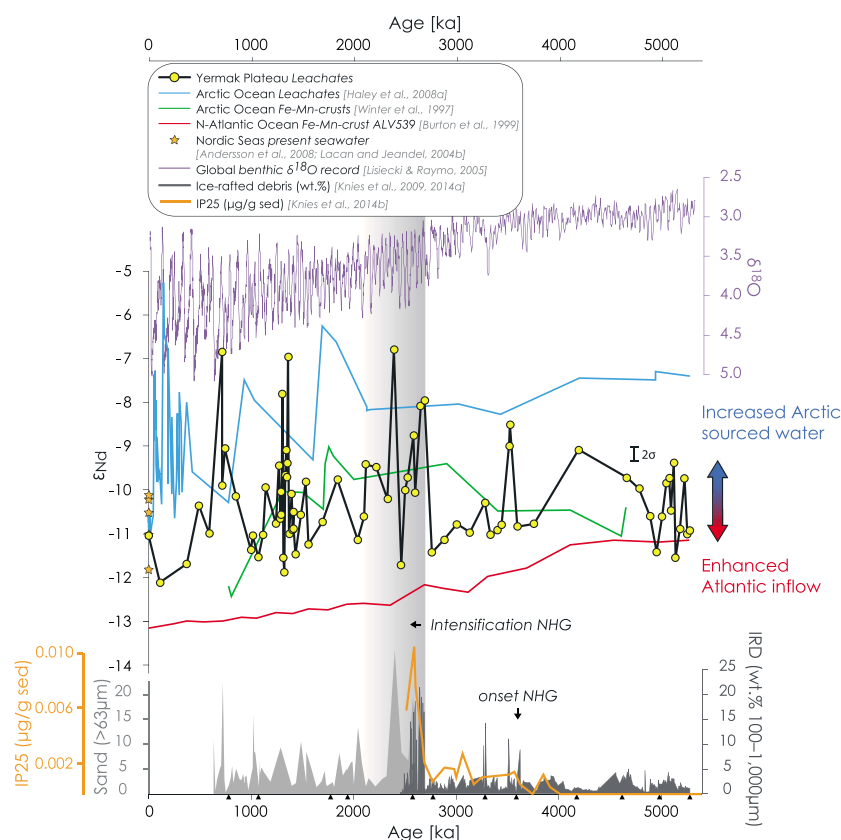
Figure 3. Comparison of the deepwater Nd isotope data of site 911 (yellow circles) with other paleo environmental records. The present-day dissolved deepwater Nd isotope compositions near site 911 are shown as orange stars [*Andersson et al.*, 2008; *Lacan and Jeandel*, 2004b]. The central Arctic Ocean intermediate water leachate data (blue line) [*Haley et al.*, 2008a], the Arctic Alpha Ridge micronodule data (green line) [*Winter et al.*, 1997], the North Atlantic Fe-Mn crust record of NADW (red line) [*Burton et al.*, 1999], the global benthic $\delta^{18}O$ stacked record (purple line), the IP25 (μg/g sed) record of site 910C (orange line) [*Knies et al.*, 2014b], and the variability of the ice-rafted debris (IRD; wt %, coarse fraction >100 μm) and sand (%, >63 μm) content of site 911A [*Knies et al.*, 2009, 2014a] are displayed. The black arrows indicate the onset of the Northern Hemisphere Glaciation (NHG) at ~3.6 Ma [*Mudelsee and Raymo*, 2005] and the major intensification of the NHG at 2.7 Ma additionally visualized as grey shading. The black triangles below the *x* axis mark the 12 age fix points of the accepted age model [*Mattingsdal et al.*, 2014; *Knies et al.*, 2014a] (Table S2).

signatures of the leachates on Yermak Plateau only varied between 18.60 and 18.75 without any significant trend ($r^2 = 0$) prior to 2.7 Ma, whereas thereafter the amplitude increased between similar baseline values near 18.6 and maximum values reaching 19.15 at 0.4 Ma (Figure 2). The $^{206}Pb/^{204}Pb$ maxima became systematically more pronounced over the past 2.7 Myr ($r^2 = 0.685$). Essentially, the same pattern was found for the $^{207}Pb/^{204}Pb$ and $^{208}Pb/^{204}Pb$ signatures of the leach fraction. The detrital fraction Pb isotope data followed the trend of the leachate data. The core top (0–3 cm ≈ last 350 years) Pb isotope signal shows a markedly less radiogenic value of 18.85 most likely due to contamination with anthropogenic lead (the $^{206}Pb/^{204}Pb$ composition of anthropogenic Pb in the Greenland Sea and Eurasian basin ranges between 17.75 and 18.38 [*Gobeil et al.*, 2001]) during the last ~100 years and will not be considered for paleoceanographic interpretation.

4. Discussion

4.1. Factors Influencing the Seawater Nd and Pb Isotope Signatures Extracted from Fe-Mn Oxyhydroxide Coatings

The ferromanganese oxyhydroxide fraction of the bulk sediments has been demonstrated to record the radiogenic isotope signal of the bottom waters. On Yermak Plateau less radiogenic ε_{Nd} values generally reflect enhanced influence of warm Atlantic waters from the south, while more radiogenic Nd isotope signatures are a consequence of enhanced influence from the Arctic region. Extracting the pure seawater-derived

Nd and Pb isotope signatures from the Fe-Mn oxyhydroxide coatings of bulk sediments can, however, be difficult in particular sedimentary settings. A decarbonation step with acetic acid prior to the HH-leach step, which is commonly part of the leaching procedure [e.g., *Gutjahr et al.*, 2007, 2008; *Piotrowski et al.*, 2008], may lead to biases, for example, at locations influenced by deposition of volcanic ashes or when carbonate contents are low [*Elmore et al.*, 2011; *Molina-Kescher et al.*, 2014]. *Wilson et al.* [2013] found that the most - reliable seawater Nd isotopic compositions are extracted from the authigenic fraction by a single reductive leaching step without decarbonation. Our core top authigenic Nd isotope signature on Yermak Plateau ($\varepsilon_{Nd} = -11.0 \pm 0.3$) was obtained applying this technique and is indistinguishable from present-day deepwater Nd isotope composition at locations proximal to the Atlantic inflow branch at 600 m water depth ($\varepsilon_{Nd} = -11.0 \pm 0.2$) [*Lacan and Jeandel*, 2004b] and at the western Svalbard margin at 1000 m water depth ($\varepsilon_{Nd} = -11.9 \pm 0.3$) [*Werner et al.*, 2014].

The $^{87}Sr/^{86}Sr$ signatures of the leached ferromanganese coatings of site 911 sediments range from 0.70891 to 0.71249 and are thus in most cases slightly more radiogenic than the global $^{87}Sr/^{86}Sr$ evolution of seawater of the past 5.2 Myr [*McArthur et al.*, 2001]. *Crocket et al.* [2013] also showed more radiogenic $^{87}Sr/^{86}Sr$ composition of the authigenic fraction than seawater in the North Atlantic Ocean partly originating from preformed coatings but concluded that the contamination of the seawater Pb isotopic composition and by inference of the Nd isotope data is negligible. This is in agreement with the mass balance considerations of *Gutjahr et al.* [2007] who demonstrated that offsets of the $^{87}Sr/^{86}Sr$ signatures of the leachates from seawater values do not allow to unambiguously constrain the reliability of the Nd isotope data of the same samples due to much higher Sr concentrations of the detrital material. The agreement of the core top leach data and the present-day seawater compositions documents the reliable extraction of seawater Nd isotope compositions from the Fe-Mn oxyhydroxide fraction at our study site without significant detrital contamination.

Our downcore data of site 911 are consistent with mixtures of water masses from the North Atlantic Ocean and Arctic Ocean. Nevertheless, variable boundary exchange processes with the shelves [*Lacan and Jeandel*, 2005b], in particular the Svalbard margin, may have played a role in this area and may have contributed to some of the peaks of the site 911 records. The degree to which extent boundary exchange influenced the isotopic composition of the bottom waters at the Yermak Plateau cannot be quantified but was overall low taken the present-day situation as a reference.

The correlation of the Nd and Pb isotopic compositions of the detrital fraction and of the leached seawater signatures (Figure S1) may point to some influence of partial dissolution of the detrital material in seawater, i.e., via IRD transported to our study site from a different source such as the Kara Sea or associated with preformed coatings, which originate from precipitation of Fe in the transition zones of the rivers between freshwater and salt water [*Bayon et al.*, 2004; *Kraft et al.*, 2013]. Such processes may have contributed to those peak radiogenic Nd isotope compositions coinciding with peak IRD deposition in our record (Figure 3), but large effects are unlikely, because the IRD accumulation rates were overall low. These considerations support that the isotopic compositions of the leached fraction reflect the ambient bottom water signatures and that the observed variations were predominantly a consequence of changes in the mixtures of the dominant water masses. In the following, we interpret our data accordingly.

4.2. Deep Water Mass Mixing on Yermak Plateau Over the Past 5.2 Myr

The Fram Strait is a hydrographically complex area that has undergone large changes in ocean circulation and sediment transport processes during the past 5.2 Myr [*Knies et al.*, 2002, 2009, 2014a, 2014b; *Maccali et al.*, 2012]. Generally, site 911 has been strongly influenced by water mass mixing between the Nordic Seas fed by the North Atlantic Current crossing the Iceland—Faroe—Ridge and the Arctic Ocean outflow water. The evolution of the mixing proportions of the different end-member water masses have been recorded by the Nd isotope signatures of past seawater on Yermak Plateau. Less radiogenic values indicate a generally stronger influence of the North Atlantic Current (NAC) flowing into the Nordic Seas (present-day $\varepsilon_{Nd} = -13.2$ to -13.0) [*Lacan and Jeandel*, 2004c, 2005b], especially during periods with a strong AMOC. This was the case for the period between 2 and 1.5 Ma, during which dense NADW was exported from the Nordic Seas and compensated by a strong return flow of warm water from the Atlantic Ocean [*Bell et al.*, 2015]. This enhanced inflow is clearly reflected by a relatively low amplitude of variability in the ε_{Nd} record and overall less radiogenic values at the Yermak Plateau during that period of time (Figure 3). More radiogenic values point to a stronger influence of the Arctic Ocean outflow branch through the Fram Strait which at present is characterized by an ε_{Nd} value of $= -9.5$ between 100 m and 1300 m
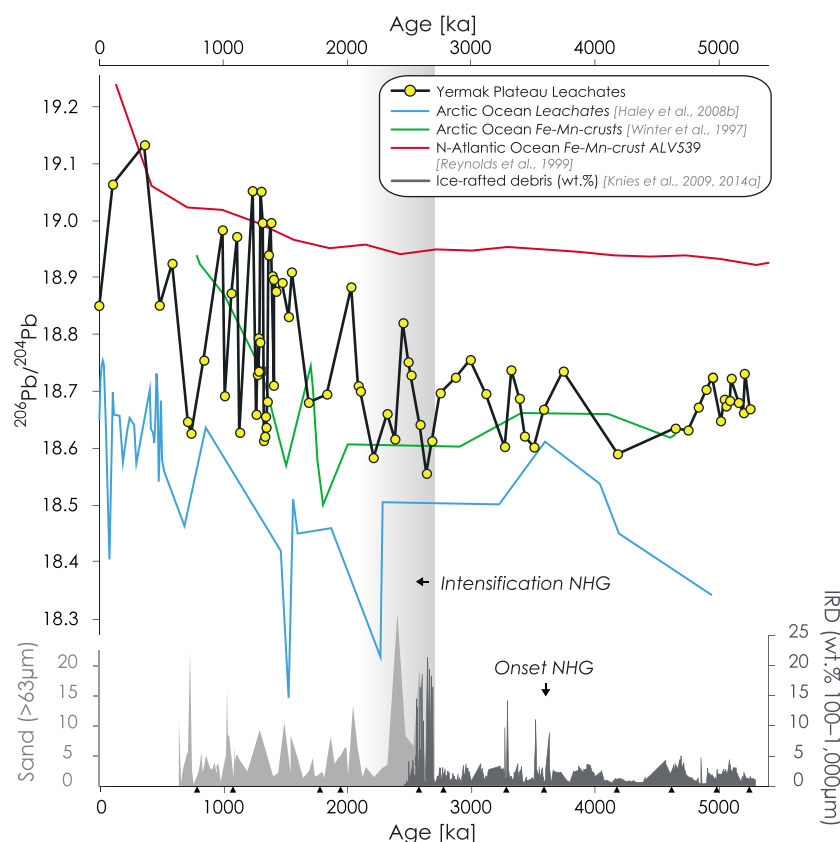
Figure 4. Comparison of the deepwater Pb isotope data of site 911 (yellow circles) with other paleo environmental records. The 2σ errors for the Pb isotope analyses are smaller than the dots. The Arctic Ocean leaches from the Lomonosov Ridge (blue line) [*Haley et al.*, 2008b], the North Atlantic Fe-Mn crust record (red line) [*Reynolds et al.*, 1999], and an Arctic diagenetic micronodules record (green line) [*Winter et al.*, 1997] and ice-rafted debris (IRD; wt %, coarse fraction >100 μm) as well as sand (%, >63 μm) content of site 911A [*Knies et al.*, 2009, 2014a] are also presented. The black arrows again indicate the onset of the Northern Hemisphere Glaciation (NHG) at ~3.6 Ma [*Mudelsee and Raymo*, 2005] and the major intensification of the NHG at 2.7 Ma additionally visualized as grey shading. The black triangles below the x axis mark the 12 age fix points [*Mattingsdal et al.*, 2014; *Knies et al.*, 2014a] (Table S2).

water depth [*Andersson et al.*, 2008] (Figure 3). During periods of enhanced Arctic outflow, sea ice extent and freshwater supply from the Arctic Ocean through Fram Strait were increased, which inhibited formation of deep water in the Nordic Seas [e.g., *Henrich et al.*, 2002]. This inference is consistent with observations by *Ganopolski and Rahmstorf* [2001] and *Clark et al.* [2002], who suggested a reduction of the thermohaline circulation during glaciations, when the amount of Atlantic Water advected to the Nordic seas is thought to have been lower than at present. *Crocket et al.* [2011] also ascribed more radiogenic glacial ε_{Nd} values at the Rockall Trough to decreased entrainment and advection of North Atlantic waters into the Nordic Seas [*Sarnthein et al.*, 1995].

The Nd isotope record of past seawater at site 911 suggests that the most pronounced change in oceanographic and climatic conditions of the past 5.2 Myr occurred at the onset of the major NHG at 2.7 Ma. Thus, we separate the discussion of the record into two time intervals: (1) the Pliocene period prior to the onset of the NHG, which was characterized by a low Nd and Pb isotope variability, and (2) the late Pliocene/Quaternary period after 2.7 Ma characterized by significantly higher amplitudes of Nd and Pb isotope variabilities extending to more radiogenic values (Figures 3 and 4) linked to the waxing and waning of the Northern Hemisphere ice sheets documented by the global deepwater δ^{18}O record [*Lisiecki and Raymo*, 2005].

4.2.1. The Pliocene Record (5.2 to 2.7 Ma)
The early part of the record comprises the more stable and warmer climatic conditions of the middle to early Pliocene, which was characterized by smaller polar ice sheets and higher deep-sea temperatures [e.g., *Sarnthein et al.*, 2009]. The deepwater Nd isotope composition on Yermak Plateau varied only moderately during

the Zanclean/early Pliocene (5.2–3.6 Ma), consistent with the ice-free conditions over the Yermak Plateau until 3.9 Ma indicated by the absence of the sea ice biomarker IP_{25} [*Belt and Müller*, 2013; *Knies et al.*, 2014b]. The ε_{Nd} signatures of site 911 were similar to contemporaneous NADW, in particular during the oldest period of our record between 5.2 and 4.8 Ma indicating an efficient exchange of water masses between the Arctic and Atlantic basins. This water mass exchange is not visible from the Nd isotope composition of Arctic Intermediate Water derived from central Arctic Ocean sediments pointing to very stable climatic conditions and a reduced influence of Atlantic waters in the Arctic basin between 8 and 2 Ma [*Haley et al.*, 2008a]. Thus, most probably any enhanced inflow of Atlantic water did not reach as far as the central Arctic basin but is only evident on the Yermak Plateau. Our data also support diminished sea ice coverage during warm periods documented by the low amount of the organic sea ice proxy IP_{25} until 3.0 Ma [*Knies et al.*, 2014b] (Figure 3).

Relatively stable climatic and oceanographic conditions from ~3.3 to 2.7 Ma including the Pliocene climate optimum from 3.29 to 2.97 Ma [*Dowsett et al.*, 2012, 2013] are indicated by the low-amplitude variability in the Pb isotope and in particular the ε_{Nd} records, which was characterized by relatively unradiogenic values consistent with a strong inflow of warm Atlantic waters and low contributions of water masses from the Arctic Ocean. This is also supported by the difference (~1 ε_{Nd} unit) of the Yermak Plateau ε_{Nd} signatures to those of NADW in the western North Atlantic [*Burton et al.*, 1999; *O'Nions et al.*, 1998], which is smaller than the modern day difference (~2.5 ε_{Nd} unit). These observations are in agreement with the low sea ice variability and occurrence of only first-year sea ice similar to the modern (summer) conditions indicated by IP_{25} prior to 2.7 Ma [*Knies et al.*, 2014a].

4.2.2. 2.7 Ma to Present

After 2.7 Ma ocean circulation and Arctic sea ice coverage [*Stein and Fahl*, 2013], as well as erosional input in the Nordic Seas, changed significantly, resulting in enhanced glacial/interglacial variability in the isotopic records. The movement of the Arctic front [*Hennissen et al.*, 2014] and pronounced waxing and waning of the ice sheets and sea ice extent were the main mechanisms changing the water mass exchange and sediment transport at the Yermak Plateau. The seawater Nd isotope record at site 911 shows a significant transient peak of 3.5 ε_{Nd} units to more radiogenic values at 2.7 Ma (MIS G6/4; Figure 2), indicating a major modification of water mass exchange, which lasted for at least 100 kyr. The more radiogenic signal in our record was a consequence of an increased Arctic influence on the Yermak Plateau, which was enabled by a southward shift of the Arctic front and weakening of the NAC inflow into the Nordic Seas [*Hennissen et al.*, 2014]. These authors further described cooler conditions and fresher water masses in the North Atlantic Ocean at around 2.74 Ma. The signal may also have been introduced as a consequence of the first ice sheet in the northern Barents Sea reaching the shelf edge [*Knies et al.*, 2014a] and of the establishment of modern sea ice conditions on the Yermak Plateau, which is supported by a gradual increase in IP_{25} concentrations [*Knies et al.*, 2014b]. Enhanced brine formation near the edges of these extended ice sheets during glacial periods, in particular in the Kara Sea area [*Haley et al.*, 2008a; *Chen et al.*, 2012], likely contributed to the more radiogenic Nd isotope compositions of the bottom waters on the Yermak Plateau at that time.

Unlike the North Atlantic [e.g., *Reynolds et al.*, 1999] and the central Arctic Ocean [*Winter et al.*, 1997; *Haley et al.*, 2008a] an overall trend to less radiogenic ε_{Nd} values of deep waters since the onset of the NHG did not occur at site 911 on Yermak Plateau after 2.7 Ma. Records of North Atlantic Deep Water (NADW) in the northwestern Atlantic [*Burton et al.*, 1999], as well as on the Lomonosov Ridge in the central Arctic Ocean (IODP leg 302, "ACEX"), showed a post-NHG long-term trend toward less radiogenic ε_{Nd} signatures [*Haley et al.*, 2008a]. The main reason for the absence of the trend in the Yermak Plateau record is most likely that the mechanisms causing these trends in the North Atlantic and intermediate-depth Arctic Ocean played no or only a subordinate role on the Yermak Plateau. The influence of the Arctic signatures on Yermak Plateau has, however, been outcompeted by the prevailing admixture of warm Atlantic water from the Nordic Seas which must have experienced a different Nd isotope evolution. The trends to less radiogenic Nd and more radiogenic Pb isotope values recorded in ferromanganese crusts from the NW Atlantic were caused by either a change in the provenance of sediment supply or an increase in the weathering contributions of older continental rocks in the Baffin Bay/Labrador Sea region [*Reynolds et al.*, 1999]. This mechanism did not significantly influence the Nd and Pb isotope signatures on Yermak Plateau because waters originating in the Labrador Sea were most likely mainly flowing westward and southward [*Lacan and Jeandel*, 2004c].

Three further distinct highly radiogenic seawater Nd isotope peaks at ~2.4 Ma, ~1.4 Ma, and ~0.7 Ma were found (Figure 3). These peaks are also inferred to reflect increased contributions from highly radiogenic

source waters supplied via brine formation near the Eurasian shelf in the Kara Sea region. This region is fed by weathering products of the Putorana flood basalts during glacial periods with ice sheets on Siberia extending until the Kara Sea region similar to glacial marine oxygen isotope stage (MIS) 6 [*Haley et al.*, 2008a]. The radiogenic Nd isotope signatures of the bottom waters above Yermak Plateau were thus most likely a consequence of the outflow of highly radiogenic waters from the Arctic Ocean, assuming that the inflowing Atlantic waters were at the same time strongly reduced [*Haley et al.*, 2008a]. The Nd isotopic signature on the Eurasian shelf, in particular in the Kara Sea, is largely controlled by the drainage of the Ob (ε_{Nd}~ −6) and Yenisei Rivers (ε_{Nd}~ −5) [*Porcelli et al.*, 2009]. The ε_{Nd} values on the Eurasian shelf in the Kara Sea region thus reflect a mixture of contributions from (1) the Yenisei River which obtains its Nd isotope signature dominantly from weathering of the rocks of the Siberian flood basalt province (ε_{Nd} = 0 to +2.9) [*Sharma et al.*, 1992], the Sayan Mountains (ε_{Nd} = −5 to +3) [*Vorontsov et al.*, 2010], and rocks of Precambrian age in the lower part of the rivers and (2) the Ob River, which carries a mixture of the signatures of the West Siberian Lowland, the Altai Mountains, and the Ural Mountains (ranging from −6 to +8.4 ε_{Nd}) [*Chen and Jahn*, 2002].

Apart from enhanced brine formation, the younger radiogenic peaks can thus at least partly be explained by preformed coatings, which contain the highly radiogenic Nd isotope signal from the Siberian rivers and shelves and were transported to the Yermak Plateau as IRD incorporated in icebergs and sea ice via the Transpolar Drift (TPD) [*Tütken et al.*, 2002; *Pfirman et al.*, 1997]. A role of dissolving IRD cannot be completely excluded, but a large effect is not expected due to the low IRD accumulation rates.

Another hypothesis to explain the radiogenic Nd isotope peaks in the seawater record is boundary exchange with Icelandic basalts. For glacial periods severe reductions of the Atlantic MOC [*Ganopolski and Rahmstorf*, 2001; *Clark et al.*, 2002] or even shutdowns due to the enhanced freshwater input from the Arctic Ocean have been reported [*Peterson et al.*, 2006]. During those times the Nordic Sea waters may have become more radiogenic caused by boundary exchange with the basaltic margin of the Norwegian Sea basin including Iceland, Jan Mayen, and the Faroe Islands. This boundary exchange may have led to much more radiogenic glacial deep waters in the Norwegian basin [*Lacan and Jeandel*, 2004b, and references therein] and further downstream at the Yermak Plateau. However, we consider this second hypothesis rather unlikely, because the radiogenic Nd isotope signal needs to be transported over a very long distance from Iceland to the Yermak Plateau (~2000 km), for which there is currently no evidence. In contrast, there are numerous studies documenting the transport of waters and sediment from the Arctic Ocean to the Yermak Plateau, e.g., via the Transpolar Drift [*Pfirman et al.*, 1997; *Tütken et al.*, 2002; *Knies et al.*, 2002, 2009; *Junttila et al.*, 2008; *Maccali et al.*, 2012].

4.3. Sediment Transport on the Yermak Plateau Based on Nd and Pb Isotopes

It has been inferred that the detrital sediments deposited on Yermak Plateau have been dominated by contributions from Svalbard (ε_{Nd} values ranging between −3.3 in the western part [*Peucat et al.*, 1989] and −21 in the northern part [*Johansson and Gee*, 1999]), as well as sediments from Bear Island and the Norwegian shelf from the south (ε_{Nd} values = −15.1 to −10.1 [*Farmer et al.*, 2003]) (Figure 5). This is supported by seismic profiles [*Geissler et al.*, 2011; *Mattingsdal et al.*, 2014] showing the predominant deposition of contourites (from a southern source) on Yermak Plateau prior to 2.7 Ma. Our data of site 911 indicate a small but significant switch in the sources of the detrital sediments from Bear Island and Svalbard toward increasing contributions from the Arctic Ocean, in particular from the Eurasian shelf (Kara/Laptev Sea), as well as possibly Novaya Zemlya (average ε_{Nd} = −6.4) and Franz Josef Land (ε_{Nd} = −9.5) [*Tütken et al.*, 2002] after 2.7 Ma. The latter authors for example calculated variable sediment contributions from the Eurasian shelf of 30–95% and of 5–70% from Svalbard over the past 140 ka. The change to enhanced contributions from the Arctic Ocean is documented by the shift from less radiogenic values (ε_{Nd} = −12.9 to −11.4, mean = −12.2) prior to the iNHG to more radiogenic signatures (ε_{Nd} = −12.2 to −8.4, mean = −10.7) afterward (Figure 5), coinciding with the establishment of modern winter maximum sea ice coverage at 2.7 Ma [*Knies et al.*, 2014b]. Changes in the sediment sources are supported by two distinct periods at 0.7 and 2.7 Ma, during which the most radiogenic ε_{Nd} and least radiogenic Sr isotope signatures of the detrital fraction occurred (Figures 2 and 5). These periods reveal the closest correspondence and thus highest contributions of the sediments originating from the Kara Sea and coincided with the most radiogenic glacial seawater Nd isotope compositions (Figure 5). These sediments from the Kara and Laptev Seas were most likely transported by ice via the Siberian branch of the Transpolar Drift. Moreover, our data indicate that the influence of the more radiogenic Kara Sea sediments dominated over those from the Laptev Sea during these
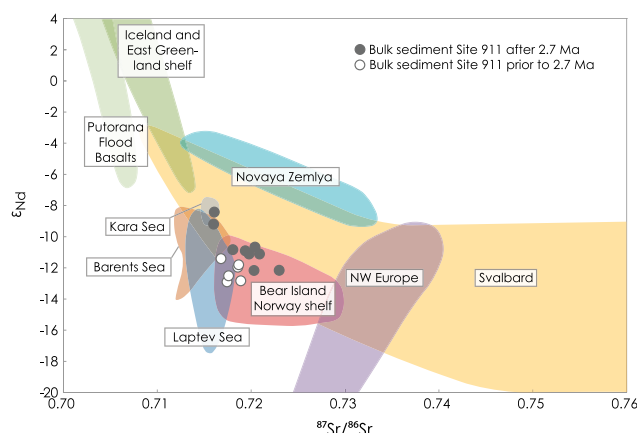
Figure 5. Comparison of the Nd and Sr isotopic compositions of the detrital sediment fraction of site 911 (black dots = younger than 2.7 Ma; open dots = prior to 2.7 Ma) with possible sediment sources. Colored arrays display the areas as follows: light green = Norilsk/Putorana food basalts [*Sharma et al.*, 1992]; blue = Kara and Laptev Sea sources [*Eisenhauer et al.*, 1999]; turquoise = Novaya Zemlya [*Tütken et al.*, 2002]; brown = Barents Sea; and Franz Josef Land [*Tütken et al.*, 2002]; yellow = Svalbard bedrocks [*Peucat et al.*, 1989; *Johansson and Gee*, 1999]; dark green = Iceland and the East Greenland shelf (basaltic); red = sediments from Bear Island and Norwegian shelf [*Farmer et al.*, 2003]; and lavender = NW Europe including British Isles, Scandinavia, and the Norwegian Sea [*Farmer et al.*, 2003].

periods. The elevated smectite content found at site 911 today [*Wahsner et al.*, 1999], but especially prior to 2.7 Ma [*Knies et al.*, 2009], supports the importance of sediment supply from the Kara Sea transported via the TPD.

The bulk detrital sediment Pb isotope signatures of site 911 are overall similar to those in the central Arctic Ocean [*Winter et al.*, 1997; *Haley et al.*, 2008b] (Figure 6), which have mainly been derived from the Siberian shelves. The sediments on Yermak Plateau have been slightly more radiogenic in their Pb isotope compositions than bulk sediment originating from the Siberian flood basalts [*Sharma et al.*, 1992] and Svalbard bedrocks [*Ionov et al.*, 2002]. Prior to 2.7 Ma the Pb isotope compositions of site 911 sediments were more similar to those of the bulk rocks of Bear Island [*Farmer et al.*, 2003] and Svalbard [*Ionov et al.*, 2002] (Figure 6). After 2.7 Ma the Pb isotope compositions of the sediments became more

radiogenic, consistent with enhanced contributions of Siberian material from the Eurasian shelf. Similar to the Nd isotopic composition, the Pb isotopic signal indicates that Franz Josef Land [*Levskii et al.*, 2006] may also have been an important source of sediment.

4.4. Changes in Weathering Regime and Sediment Sources Over the Past 5.2 Ma: Pb Isotope Evidence

Prior to the onset of Northern Hemisphere Glaciation the Pb isotope composition on the Yermak Plateau was characterized by consistent unradiogenic values and a low variability (Figure 2) due to the limited extent of ice sheets, which resulted in more congruent weathering of the Pb isotopes and signatures similar to the bulk detrital signal [*von Blanckenburg and Nägler*, 2001]. The low variability and more congruent and invariant Pb isotope signatures of Yermak Plateau seawater are similar to records from the Arctic [*Winter et al.*, 1997; *Haley et al.*, 2008b] and Atlantic Oceans [*Reynolds et al.*, 1999] (Figure 4) and were mainly caused by largely stable nonglacial weathering conditions. The low extent of the continental ice cover on the Northern Hemisphere prior to 2.7 Ma implies that the Pb was mainly released by chemical weathering of older and deeply weathered soils due to the warm temperatures during the Pliocene. The relatively unradiogenic Pb isotope record prior to 2.7 Ma thus indicates essentially constant erosional supply of material, most likely from Svalbard to the Yermak Plateau.

After 2.7 Ma a major buildup of the Northern Hemisphere ice sheets occurred, sea ice expanded to modern maximum winter conditions [*Knies et al.*, 2014b], and the weathering conditions changed significantly resulting in a twofold to threefold decrease in chemical weathering rates during glacial periods [*Foster and Vance*, 2006]. In contrast, mechanical erosion intensity increased leading to enhanced exposure of fresh mineral surfaces, which led to the predominant release of radiogenic ^{206,207,208}Pb (incongruent weathering) [*von Blanckenburg and Nägler*, 2001; *Foster and Vance*, 2006] from the old continental rocks of Greenland and parts of Svalbard. The significantly enhanced amplitude and overall increase of the radiogenic Pb isotope ratios of past deep waters on Yermak Plateau after 2 Ma is consistent with that of seawater Pb isotope compositions leached from central Arctic Ocean sediments on the Lomonosov Ridge (though less pronounced) [*Haley et al.*, 2008b]. The overall gradual shift of the ^{206,207,208}Pb/^{204}Pb record to more radiogenic values on Yermak Plateau after 2.7 Ma resembles the Pb isotope evolution of the deep Canadian Basin of the Arctic Ocean recorded by sedimentary ferromanganese micronodules [*Winter et al.*, 1997] and ferromanganese crusts [*Dausmann et al.*, 2015] and the Pb isotope
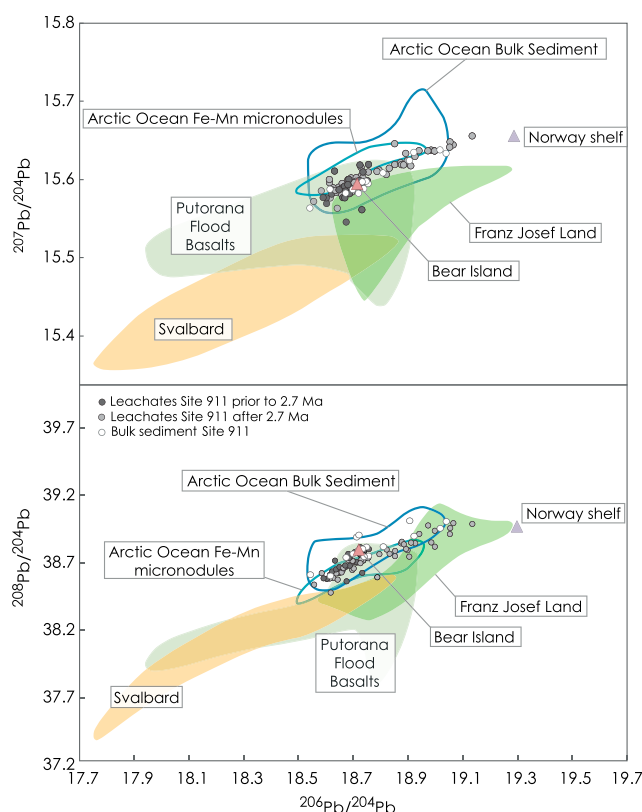
Figure 6. Radiogenic Pb isotope comparison of leachates (black dots = prior to 2.7 Ma; light grey dots = after 2.7 Ma) and detrital sediments (open dots) of site 911 with possible sources. The blue framed arrays are the bulk sediment [*Winter et al.*, 1997; *Haley et al.*, 2008b] and Fe-Mn micronodules from the Arctic Ocean [*Winter et al.*, 1997]. For comparison, the isotopic compositions of the rocks of the volcanic Franz Josef Archipelago [*Levskii et al.*, 2006], the Putorana flood basalts [*Sharma et al.*, 1992], the Norway shelf, Bear Island [*Farmer et al.*, 2003], and Svalbard rocks [*Ionov et al.*, 2002] are shown.

evolution of North Atlantic Deep Water in the western North Atlantic [*Burton et al.*, 1999; *Reynolds et al.*, 1999] indicating similar weathering and input processes. This major shift to more radiogenic values apparently occurred at different times varying between 1.7 Ma [*Winter et al.*, 1997] and after 1 Ma [*Haley et al.*, 2008b; *Reynolds et al.*, 1999] (Figure 4), which may originate from differences in sediment supply pathways and in exposed lithologies. That is, freshly exposed old granitic rocks release the most radiogenic Pb during incipient deglacial chemical weathering. Our data show that Pb released via incongruent weathering mostly contributed to the radiogenic peaks in the seawater Pb isotope record, which are systematically more radiogenic than the detrital fraction, whereas the closely corresponding changes of the Pb isotopic composition of the seawater and detrital fraction of the remainder of the record point to a change in the source area of the detrital material.

5. Conclusions

This study reconstructs the evolution of water mass mixing and erosional input on the Yermak Plateau over the past 5.2 Myr on the basis of seawater Nd and Pb isotope compositions extracted from authigenic ferromanganese oxyhydroxide coatings, as well as of the detrital fraction of ODP site 911 sediments. The Nd isotope record of past seawater did not undergo a significant trend on the Yermak Plateau, suggesting that this location has been dominantly influenced by variable amounts of modified Atlantic water advected from the Nordic Seas over the past 5.2 Ma. Two periods with distinctly different conditions are evident in the Nd isotope record. An early period, prior to the major intensification of the Northern Hemisphere Glaciation near 2.7 Ma, was characterized by less variable water mass compositions, as well as essentially invariant sediment supplies from Svalbard and the Arctic Ocean. After 2.7 Ma the environmental conditions have been characterized by higher-amplitude ε_{Nd} variability of both deep waters and detrital sediments, presumably as a result of enhanced glacial/interglacial contrasts despite that particular glacial and interglacial stages cannot be distinguished due to the limited age control as a consequence of absent carbonate. This higher variability is interpreted to be a consequence of the enhanced climatic changes reflected by the waxing and waning of ice sheets located on the Eurasian shelf and the associated supply of sea ice laden with sediments and their partial dissolution. Short periods characterized by significantly more radiogenic ε_{Nd} signatures of deep waters on Yermak Plateau such as at 2.7 Ma were driven by stronger influence of more radiogenic Arctic waters as a consequence of either brine formation near the Eurasian shelf, possibly amplified partial dissolution of radiogenic IRD from the Kara Sea, and a contemporaneous significant reduction of the Atlantic water inflow. The detrital Nd and Pb isotope compositions of the sediments from site 911 indicate dominant sediment supply from Svalbard and Bear Island and decreased influence of material from the Arctic Ocean prior to 2.7 Ma, whereas the contribution of sediments from the Kara Sea region increased after the iNHG.

Similar to the Nd isotopes, the seawater Pb isotope record shows low variability and supports a constant sediment supply prior to 2.7 Ma, dominantly from Svalbard. After 2.7 Ma and in particular after 2.0 Ma, the increasing amplitude of the isotope signatures on glacial/interglacial time scales is ascribed to enhanced glacial weathering and the waxing and waning of ice sheets, as well as changes in sea ice transport. Contrary to Nd isotopes, the seawater Pb isotope record, in particular the radiogenic Pb isotope maxima, shows a clear overall trend toward more radiogenic values after 2.7 Ma, reflecting a change in the source area of the detrital material, which was amplified by enhanced incongruent glacial release of radiogenic Pb during peak weathering of old continental rocks of Greenland and parts of Svalbard.

References

Aagaard, K., J. H. Swift, and E. C. Carmack (1985), Thermohaline circulation in the Arctic Mediterranean Seas, *J. Geophys. Res.*, *90*, 4833–4846, doi:10.1029/JC090iC03p04833.

Abouchami, W., S. J. G. Galer, and A. Koschinski (1999), Pb and Nd isotopes in NE Atlantic Fe-Mn crusts: Proxies for trace metal paleosources and paleocean circulation, *Geochim. Cosmochim. Acta*, *63*, 1489–1505.

Albarède, F., P. Telouk, J. Blichert-Toft, M. Boyet, A. Agranier, and B. Nelson (2004), Precise and accurate isotopic measurements using multiple-collector ICPMS, *Geochim. Cosmochim. Acta*, *68*, 2725–2744.

Andersson, P., D. Porcelli, M. Frank, G. Björk, R. Dahlqvist, and Ö. Gustafsson (2008), Neodymium isotopes in seawater from the Barents Sea and Fram Strait Arctic-Atlantic gateways, *Geochim. Cosmochim. Acta*, *72*, 2854–2867.

Arsouze, T., J.-C. Dutay, F. Lacan, and C. Jeandel (2009), Reconstructing the Nd oceanic cycle using a coupled dynamical-biogeochemical model, *Biogeosciences*, *6*, 2829–2846.

Barrat, J. A., F. Keller, J. Amosse, R. N. Taylor, R. W. Nesbitt, and T. Hirata (1996), Determination of rare earth elements in sixteen silicate reference samples by ICP-MS after Tm addition and ion exchange separation, *Geostand. Newsl.*, *20*, 133–139.

Bartoli, G., M. Sarnthein, M. Weinelt, H. Erlenkeuser, D. Garbe-Schönberg, and D. Lea (2005), Final closure of Panama and the onset of Northern Hemisphere Glaciation, *Earth Planet. Sci. Lett.*, *237*, 33–44.

Bayon, G., C. R. German, R. M. Boella, J. A. Milton, R. N. Taylor, and R. W. Nesbitt (2002), An improved method for extract in marine sediment fractions and its application to Sr and Nd isotopic analysis, *Chem. Geol.*, *187*, 179–199.

Bayon, G., C. R. German, K. W. Burton, R. W. Nesbitt, and N. Rogers (2004), Sedimentary Fe–Mn oxyhydroxides as paleoceanographic archives and the role of aeolian flux in regulating oceanic dissolved REE, *Earth Planet. Sci. Lett.*, *224*, 477–492.

Bell, D. B., S. J. A. Jung, and D. Kroon (2015), The Plio-Pleistocene development of Atlantic deep-water circulation and its influence on climate trends, *Quat. Sci. Rev.*, *123*, 265–282.

Belt, S. T., and J. Müller (2013), The Arctic sea ice biomarker IP$_{25}$: A review of current understanding, recommendations for future research and applications in palaeo sea ice reconstructions, *Quat. Sci. Rev.*, *79*, 9–15.

Böhm, E., J. Lippold, M. Gutjahr, M. Frank, P. Blaser, B. Antz, J. Fohlmeister, N. Frank, M. B. Andersen, and M. Deiniger (2015), Strong and deep Atlantic meridional overturning circulation during the last glacial cycle, *Nature*, *517*, 73–76.

Boyle, E. A. (1988), Vertical oceanic nutrient fractionation and glacial/interglacial CO_2 cycles, *Nature*, *331*, 55–56.

Brinkhuis, H., et al. (2006), Episodic fresh surface waters in the Eocene Arctic Ocean, *Nature*, *441*, 606–609.

Broecker, W. S., and T.-H. Peng (1982), *Tracers in the Sea*, Lamont-Doherty Geol. Obs., Palisades, New York.

Broecker, W. S., C. Rooth, and T.-H. Peng (1985), Ventilation of the deep Northeast Atlantic, *J. Geophys. Res.*, *90*, 6940–6944, doi:10.1029/JC090iC04p06940.

Burton, K. W., D.-C. Lee, J. N. Christensen, A. N. Halliday, and J. R. Hein (1999), Actual timing of neodymium isotopic variations recorded by Fe–Mn crusts in the western North Atlantic, *Earth Planet. Sci. Lett.*, *171*, 149–156.

Cane, M. A., and P. Molnar (2001), Closing of the Indonesian seaway as precursor to east African aridification around 3–4 million years ago, *Nature*, *411*, 157–162.

Chen, B., and B.-M. Jahn (2002), Geochemical and isotopic studies of the sedimentary and granitic rocks of the Altai orogen of northwest China and their tectonic implications, *Geol. Mag.*, *139*, 1–13.

Chen, T., M. Frank, B. A. Haley, M. Gutjahr, and R. Spielhagen (2012), Variations of North Atlantic inflow to the central Arctic Ocean over the last 14 million years inferred from hafnium and neodymium isotopes, *Earth Planet. Sci. Lett.*, *353–354*, 82–92.

Clark, P. U., N. G. Pisias, T. F. Stocker, and A. J. Weaver (2002), The role of the thermohaline circulation in abrupt climate change, *Nature*, *415*, 863–869.

Crocket, K. C., D. Vance, M. Gutjahr, G. L. Foster, and D. A. Richards (2011), Persistent Nordic deep-water overflow to the glacial North Atlantic, *Geology*, *39*, 515–518, doi:10.1130/G31677.1.

Crocket, K. C., G. L. Foster, D. Vance, D. A. Richards, and M. Tranter (2013), A Pb isotope tracer of ocean-ice sheet interaction: the record from the NE Atlantic during the Last Glacial/Interglacial cycle, *Quat. Sci. Rev.*, *82*, 133–144.

Dausmann, V., M. Frank, C. Siebert, M. Christl, and J. R. Hein (2015), The evolution of climatically driven weathering inputs into the western Arctic Ocean since the late Miocene: Radiogenic isotope evidence, *Earth Planet. Sci. Lett.*, *419*, 111–124.

De Menocal, P. B., D. W. Oppo, R. G. Fairbanks, and W. L. Prell (1992), Pleistocene δ^{13}C variability of North Atlantic intermediate water, *Paleoceanography*, *7*, 229–250, doi:10.1029/92PA00420.

De Schepper, S., J. Groeneveld, B. D. A. Naafs, C. Van Renterghem, J. Hennissen, M. J. Head, S. Louwye, and K. Fabian (2013), Northern Hemisphere glaciation during the globally warm early late Pliocene, *PLoS One 8(12)*, e81508.

De Schepper, S., M. Schreck, K. M. Beck, J. Matthiessen, K. Fahl, and G. Mangerud (2015), Early Pliocene onset of modern Nordic Seas circulation related to ocean gateway changes, *Nat. Commun.*, *6*, 8659.

Dowsett, H. J., et al. (2012), Assessing confidence in Pliocene sea surface temperatures to evaluate predictive models, *Nat. Clim. Change*, *2*, 365–371.

Dowsett, H. J., et al. (2013), Sea surface temperature of the mid-Piacenzian Ocean: A data model comparison, *Sci. Rep.*, *3*, 2013.

Driscoll, N. W., and G. H. Haug (1998), A short-circuit in thermohaline circulation: A cause for northern hemisphere glaciation?, *Science*, *282*, 436–438.

Eisenhauer, A., H. Meyer, V. Rachold, T. Tütken, B. Wiegand, B. T. Hansen, R. F. Spielhagen, F. Lindeman, and H. Kassens (1999), Grain size separation and sediment mixing in Arctic Ocean sediments: Evidence from the strontium isotope systematic, *Chem. Geol.*, *158*, 173–188.

Eldrett, J. S., I. C. Harding, P. A. Wilson, E. Butler, and A. P. Roberts (2007), Continental ice in Greenland during the Eocene and Oligocene, *Nature*, *446*, 176–179.

Elmore, A. C., A. M. Piotrowski, J. D. Wright, and A. E. Wright (2011), Testing the extraction of past seawater Nd isotopic composition from North Atlantic deep sea sediments and foraminifera, *Geochem. Geophys. Geosyst.*, *12*, Q09008, doi:10.1029/2011GC003741.

Erel, Y., Y. Harlavan, and J. D. Blum (1994), Lead isotope systematics of granitoid weathering, *Geochim. Cosmochim. Acta*, *58*, 5299–5306.

Farmer, G. L., D. Barber, and J. Andrews (2003), Provenance of late Quaternary ice-proximal sediments in the North Atlantic: Nd, Sr and Pb isotopic evidence, *Earth Planet. Sci. Lett.*, *209*, 227–243.

Foster, G. L., and D. Vance (2006), Negligible glacial–interglacial variation in continental chemical weathering rates, *Nature*, *444*, 918–921.

Frank, M. (2002), Radiogenic isotopes: Tracers of past ocean circulation and erosional input, *Rev. Geophys.*, *40*(1), 1001, doi:10.1029/2000RG000094.

Frank, M., B. C. Reynolds, and R. K. O'Nions (1999), Nd and Pb isotopes in Atlantic and Pacific water masses before and after closure of the Panama gateway, *Geology*, *27*, 1147–1150.

Fronval, T., and E. Jansen (1996), Late Neogene paleoclimates and paleoceanography in the Iceland-Norwegian Sea: Evidence from the Iceland and Vøring Plateaus, in *Proceedings of the Ocean Drilling Program*, *Sci. Results*, vol. 151, edited by J. Thiede et al., pp. 455–468 , Ocean Drill. Program, College Station, Tex.

Ganopolski, A., and S. Rahmstorf (2001), Rapid changes of glacial climate simulated in a coupled climate model, *Nature*, *409*, 153–158.

Geissler, W. H., W. Jokat, and H. Brekke (2011), The Yermak Plateau in the Arctic Ocean in the light of reflection seismic data—Implication for its tectonic and sedimentary evolution, *Geophys. J. Int.*, *187*, 1334–1362.

Gobeil, C., R. W. Macdonald, J. N. Smith, and L. Beaudin (2001), Atlantic water flow pathways revealed by lead contamination in Arctic Basin sediments, *Science*, *293*, 1301–1304.

Goldstein, S. L., S. R. Hemming, D. H. Heinrich, and K. T. Karl (2003), Long-lived isotopic tracers in oceanography, paleoceanography, and ice-sheet dynamics, in *Treatise on Geochemistry*, pp. 453–485, Pergamon, Oxford, U. K.

Gordienko, P. A., and A. F. Laktionov (1969), Circulation and physics of the Arctic basin waters, in *Annals of the International Geophysical Year*, vol. 46, edited by A. L. Gordon and F. W. G. Baker, pp. 94–112 , Pergamon, New York.

Grøsfjeld, K., S. de Schepper, K. Fabian, K. Husum, S. Baranwal, K. Andreassen, and J. Knies (2014), Dating and palaeoenvironmental reconstruction of early Pliocene sediments from the Yermak Plateau ODP Hole 911A in the Arctic Ocean, NNW of Svalbard, based on marine palynology, *Palaeogeogr. Palaeoclimatol. Palaeoecol.*, *414*, 382–402.

Gutjahr, M., and J. Lippold (2011), Early arrival of southern source water in the deep North Atlantic prior to Heinrich event 2, *Paleoceanography*, *26*, PA2101, doi:10.1029/2011PA002114.

Gutjahr, M., M. Frank, C. H. Stirling, V. Klemm, T. van de Flierdt, and A. N. Halliday (2007), Reliable extraction of a deep water trace metal isotope signal from Fe-Mn oxyhydroxide coatings of marine sediments, *Chem. Geol.*, *242*, 351–370.

Gutjahr, M., M. Frank, C. H. Stirling, L. D. Keigwin, and A. N. Halliday (2008), Tracing the Nd isotope evolution of North Atlantic deep and intermediate waters in the western North Atlantic since the Last Glacial Maximum from Blake Ridge sediments, *Earth Planet. Sci. Lett.*, *266*, 61–77.

Gutjahr, M., M. Frank, A. N. Halliday, and L. D. Keigwin (2009), Retreat of the Laurentide ice sheet tracked by the isotopic composition of Pb in western North Atlantic seawater during termination 1, *Earth Planet. Sci. Lett.*, *286*, 546–555.

Haley, B. A., and L. Polyak (2013), Pre-modern Arctic Ocean circulation from surface sediment neodymium isotopes, *Geophys. Res. Lett.*, *40*, 893–897, doi:10.1002/grl.50188.

Haley, B. A., M. Frank, R. F. Spielhagen, and A. Eisenhauer (2008a), Influence of brine formation on Arctic Ocean circulation over the past 15 million years, *Nat. Geosci.*, *1*, 68–72.

Haley, B. A., M. Frank, R. F. Spielhagen, and J. Fietzke (2008b), Radiogenic isotope record of Arctic Ocean circulation and weathering inputs of the past 15 million years, *Paleoceanography*, *23*, PA1S13, doi:10.1029/2007PA001486.

Hansen, B., and S. Østerhus (2000), North Atlantic-Nordic Seas exchanges, *Prog. Oceanogr.*, *45*, 109–208.

Haug, G. H., and R. Tiedemann (1998), Effect of the formation of the Isthmus of Panama on Atlantic Ocean thermohaline circulation, *Nature*, *393*, 673–676.

Hemming, S. R. (2004), Heinrich events: Massive Late Pleistocene detritus layers of the North Atlantic and their global climate imprint, *Rev. Geophys.*, *42*, RG1005, doi:10.1029/2003RG000128.

Hennissen, J. A. I., M. J. Head, S. De Schepper, and J. Groeneveld (2014), Palynological evidence for a southward shift of the North Atlantic current at ~2.6 Ma during the intensification of the late Cenozoic Northern Hemisphere glaciation, *Paleoceanography*, *29*, 564–580, doi:10.1002/2013PA002543.

Henrich, R., K.-H. Baumann, R. Huber, and H. Meggers (2002), Carbonate preservation records of the past 3 Myr in the Norwegian–Greenland Sea and the northern North Atlantic: Implications for the history of NADW production, *Mar. Geol.*, *184*, 17–39.

Horwitz, E. P., R. Chiarizia, and M. L. Dietz (1992), A novel strontium-selective extraction chromatographic resin, *Solvent Extr. Ion Exch.*, *10*, 313–336.

Huybers, P., and P. Molnar (2007), Tropical cooling and the onset of North American glaciation, *Clim. Past*, *3*, 549–557.

Imbrie, J., et al. (1993), On the structure and origin of major glaciation cycles 2. The 100,000-year cycle, *Paleoceanography*, *8*, 699–735, doi:10.1029/93PA02751.

Ionov, D. A., S. B. Mukasa, and J.-L. Bodinier (2002), Sr-Nd-Pb isotopic compositions of peridotite xenoliths from Spitsbergen: Numerical modeling indicates Sr-Nd decoupling in the mantle by melt percolation metasomatism, *J. Petrol.*, *43*, 2261–2278.

Jacobsen, S. B., and G. J. Wasserburg (1980), Sm-Nd isotopic evolution of chondrites, *Earth Planet. Sci. Lett.*, *50*, 139–155.

Jansen, E., and J. Sjøholm (1991), Reconstruction of glaciation over the past 6 Myr from ice-borne deposits in the Norwegian Sea, *Nature*, *349*, 600–603.

Jansen, E., T. Fronval, F. Rack, and J. E. T. Channell (2000), Pliocene-Pleistocene ice rafting history and cyclicity in the Nordic Seas during the last 3.5 Myr, *Paleoceanography*, *15*, 709–721, doi:10.1029/1999PA000435.

Jeandel, K. M., S. P. Khatiwala, S. L. Goldstein, S. R. Hemming, and T. van de Flierdt (1998), Concentrations and isotopic compositions of neodymium in the eastern Indian Ocean and Indonesian straits, *Geochim. Cosmochim. Acta*, *62*, 2597–2607.

Johansson, Å., and D. G. Gee (1999), The late Palaeoproterozoic Eskolabreen granitoids of southern Ny Friesland, Svalbard Caledonides—Geochemistry, age, and origin, *GFF*, *121*, 113–126.

Junttila, J., T. Lahtinen, and K. Strand (2008), Provenance and sea-ice transportation of mid-Pliocene and Quaternary sediments, Yermak Plateau, Arctic Ocean (ODP Site 911), *Boreas*, *37*, 273–285.

Karas, C., D. Nürnberg, A. K. Gupta, R. Tiedemann, K. Mohan, and T. Bickert (2009), Mid-Pliocene climate change amplified by a switch in Indonesian subsurface through flow, *Nat. Geosci.*, *2*, 434–438.

Karcher, M. J., and J. M. Oberhuber (2002), Pathways and modification of the upper and intermediate waters of the Arctic Ocean, *J. Geophys. Res.*, *107*(C6), 3049, doi:10.1029/2000JC000530.

Khélifi, N., and M. Frank (2014), A major change in North Atlantic Deep Water circulation 1.6 million years ago, *Clim. Past*, *10*, 1441–1451.

Khélifi, N., M. Sarnthein, M. Frank, N. Andersen, and D. Garbe-Schönberg (2014), Late Pliocene variations of the Mediterranean outflow, *Mar. Geol.*, *357*, 182–194.

Kleiven, H. F., E. Jansen, T. Fronval, and T. M. Smith (2002), Intensification of Northern Hemisphere glaciations in the circum Atlantic region (3.5-2.4)—Ice-rafted detritus evidence, *Palaeogeogr. Palaeoclimatol. Palaeoecol.*, *184*, 213–223.

Knies, J., J. Matthiessen, C. Vogt, and R. Stein (2002), Evidence of "Mid-Pliocene (~3 Ma) global warmth" in the eastern Arctic Ocean and implications for the Svalbard/Barents Sea ice sheet during the late Pliocene and early Pleistocene (~3–1.7 Ma), *Boreas*, *31*, 82–93.

Knies, J., J. Matthiessen, A. Mackensen, R. Stein, C. Vogt, T. Frederichs, and S.-I. Nam (2007), Effects of Arctic freshwater forcing on thermohaline circulation during the Pleistocene, *Geology*, *35*, 1075–1078.

Knies, J., J. Matthiessen, C. Vogt, J. S. Laberg, B. O. Hjelstuen, M. Smelror, E. Larsen, K. Andreassen, T. Eidvin, and T. O. Vorren (2009), The Plio-Pleistocene glaciation of the Barents Sea-Svalbard region: A new model based on revised chronostratigraphy, *Quat. Sci. Rev.*, *28*, 812–829.

Knies, J., et al. (2014a), Effect of early Pliocene uplift on late Pliocene cooling in the Arctic-Atlantic gateway, *Earth Planet. Sci. Lett.*, *387*, 132–144.

Knies, J., P. Cabedo-Sanz, S. T. Belt, S. Baranwal, S. Fietz, and A. Rosell-Melé (2014b), The emergence of modern sea ice cover in the Arctic Ocean, *Nat. Commun.*, *5*, 5608.

Kraft, S., M. Frank, E. C. Hathorne, and S. Weldeab (2013), Assessment of seawater Nd isotope signatures extracted from foraminiferal shells and authigenic phases of Gulf of Guinea sediments, *Geochim. Cosmochim. Acta*, *121*, 414–435.

Kuhlbrodt, T., A. Griesel, M. Montoya, A. Levermann, M. Hofmann, and S. Rahmstorf (2007), On the driving processes of the Atlantic meridional overturning circulation, *Rev. Geophys.*, *45*, RG2001, doi:10.1029/2004RG000166.

Lacan, F., and C. Jeandel (2004a), Denmark Strait water circulation traced by heterogeneity in neodymium isotopic compositions, *Deep Sea Res., Part I*, *51*, 71–82.

Lacan, F., and C. Jeandel (2004b), Neodymium isotopic composition and rare earth element concentrations in the deep and intermediate Nordic Seas: Constrains on the Iceland Scotland overflow water signature, *Geochem. Geophys. Geosyst.*, *5*, Q11006, doi:10.1029/2004GC000742.

Lacan, F., and C. Jeandel (2004c), Subpolar mode water formation traced by neodymium isotopic composition, *Geophys. Res. Lett.*, *31*, L14306, doi:10.1029/2004GL019747.

Lacan, F., and C. Jeandel (2005a), Neodymium isotopes as a new tool for quantifying exchange fluxes at the continent-ocean interface, *Earth Planet. Sci. Lett.*, *232*, 245–257.

Lacan, F., and C. Jeandel (2005b), Acquisition of the neodymium isotopic composition of the North Atlantic Deep Water, *Geochem. Geophys. Geosyst.*, *6*, Q12008, doi:10.1029/2005GC000956.

Le Fèvre, B., and C. Pin (2005), A straightforward separation scheme for concomitant Lu-Hf and Sm-Nd isotope ratio and isotope dilution analysis, *Anal. Chim. Acta*, *543*, 209–221.

Levskii, L. K., N. M. Stolbov, E. S. Bogomolov, J. M. Vasil'eva, and E. M. Makar'eva (2006), Sr-Nd-Pb isotopic systems in basalts of the Franz Josef Land Archipelago, *Geochem. Int.*, *44*, 327–337.

Lisiecki, L. E., and M. E. Raymo (2005), A Pliocene-Pleistocene stack of 57 globally distributed benthic δ^{18}O records, *Paleoceanography*, *20*, PA1003, doi:10.1029/2004PA001071.

Lugmair, G. W., and S. J. G. Galer (1992), Age and isotopic relationships among the angrites Lewis Cliff 86010 and Angra dos Reis, *Geochim. Cosmochim. Acta*, *56*, 1673–1694.

Lunt, D. J., G. L. Foster, A. M. Haywood, and E. J. Stone (2008), Late Pliocene glaciation controlled by a decline in atmospheric CO_2 levels, *Nature*, *454*, 1102–1105.

Maccali, J., C. Hillarie-Marcel, J. Carignan, and L. C. Reisberg (2012), Pb isotopes and geochemical monitoring of Arctic sedimentary supplies and water mass export through Fram Strait since the Last Glacial Maximum, *Paleoceanography*, *27*, PA1201, doi:10.1029/2011PA002152.

Martin, E. E., S. W. Blair, G. D. Kamenov, H. D. Scher, E. Bourbon, C. Basak, and D. N. Newkirk (2010), Extraction of Nd isotopes from bulk deep sea sediments for paleoceanographic studies on Cenozoic time scales, *Chem. Geol.*, *269*(3-4), 414–431.

Martin, E. E., K. G. MacLeod, A. Jiménez Berrocoso, and E. Bourbon (2012), Water mass circulation on Demerara Rise during the Late Cretaceous, *Earth Planet. Sci. Lett.*, *327–328*, 111–120.

Maslin, M. A., G. Haug, M. Sarnthein, and R. Tiedemann (1996), The progressive intensification of Northern Hemisphere Glaciation as seen from the North Pacific, *Geol. Rundsch.*, *85*, 452–465.

Mattingsdal, R., J. Knies, K. Andreassen, K. Fabian, K. Husum, K. Grøsfjeld, and S. de Schepper (2014), A new 6 Myr stratigraphic framework for the Atlantic-Arctic gateway, *Quat. Sci. Rev.*, *92*, 170–178.

McArthur, J. M., R. J. Howarth, and T. R. Bailey (2001), Strontium isotope stratigraphy: LOWESS version 3: Best fit to the marine Sr-isotope curve for 0–509 Ma and accompanying look-up table for deriving numerical age, *J. Geol.*, *109*, 155–170.

Molina-Kescher, M., M. Frank, and E. C. Hathorne (2014), Nd and Sr isotope compositions of different phases of surface sediments in the South Pacific: Extraction of seawater signatures, boundary exchange, and detrital/dust provenance, *Geochem. Geophys. Geosyst.*, *15*, 3502–3520, doi:10.1002/2014GC005443.

Moran, K., et al. (2006), The Cenozoic palaeoenvironment of the Arctic Ocean, *Nature*, *441*, 601–605.

Mudelsee, M., and M. E. Raymo (2005), Slow dynamics of the Northern Hemisphere Glaciation, *Paleoceanography*, *20*, PA4022, doi:10.1029/2005PA001153.

Myhre, A., J. Thiede, and J. A. Firth (1995), *Proceedings of the Ocean Drilling Program, Initial Rep.*, vol. 151, 951 pp., Ocean Drill. Program, College Station, Tex.

O'Nions, R. K., M. Frank, F. von Blanckenburg, and H.-F. Ling (1998), Secular variation of Nd and Pb isotopes in ferromanganese crusts from the Atlantic, Indian and Pacific Oceans, *Earth Planet. Sci. Lett.*, *155*, 15–28.

Peltier, W. R., G. Vettoretti, and M. Stastna (2006), Atlantic meridional overturning and climate response to Arctic Ocean freshening, *Geophys. Res. Lett.*, *33*, L06713, doi:10.1029/2005GL025251.

Peterson, B. J., J. McClelland, R. Curry, R. M. Holmes, J. E. Walsh, and K. Aagaard (2006), Trajectory shifts in the Arctic and Subarctic freshwater cycle, *Science*, *313*, 1061–1066.

Peucat, J. J., Y. Ohta, D. G. Gee, and J. Bernard-Griffith (1989), U-Pb, Sr and Nd evidence for Grenvillan and latest Proterozoic tectonothermal activity in the Spitsbergen Caldonides, Arctic Ocean, *Lithos*, *22*, 275–285.

Pfirman, S., R. Colony, D. Nürnberg, H. Eicken, and I. Rigor (1997), Reconstructing the origin and trajectory of drifting Arctic sea ice, *J. Geophys. Res.*, *102*, 12,575–12,586, doi:10.1029/96JC03980.

Piepgras, D. J., and G. J. Wasserburg (1987), Rare Earth element transport in the western North Atlantic inferred from Nd isotopic observations, *Geochim. Cosmochim. Acta*, *51*, 1257–1271.

Piotrowski, A. M., S. L. Goldstein, S. R. Hemming, and R. G. Fairbanks (2004), Intensification and variability of oceanic thermohaline circulation through the last deglaciation, *Earth Planet. Sci. Lett.*, *225*, 205–220.

Piotrowski, A. M., S. L. Goldstein, S. R. Hemming, and R. G. Fairbanks (2005), Temporal relationships of carbon cycle and ocean circulation at glacial boundaries, *Science*, *307*, 1933–1938.

Piotrowski, A. M., S. L. Goldstein, S. R. Hemming, R. G. Fairbanks and D. R. Zylberberg (2008), Oscillating glacial northern and southern deep water formation from combined neodymium an carbon isotopes, *Earth Planet. Sci. Lett.*, *272*, 394–405.

Piotrowski, A. M., V. K. Banakar, A. E. Scrivner, H. Elderfield, A. Galy, and A. Dennis (2009), Indian Ocean circulation and productivity during the last glacial cycle, *Earth Planet. Sci. Lett.*, *285*, 179–189.

Piotrowski, A. M., A. Galy, J. A. L. Nicholl, N. Roberts, D. J. Wilson, J. A. Clegg, and J. Yu (2012), Reconstructing deglacial North and South Atlantic deep water sourcing using foraminiferal Nd isotopes, *Earth Planet. Sci. Lett.*, *357-358*, 289–297.

Porcelli, D., P. S. Andersson, M. Baskaran, M. Frank, G. Björk, and I. Semiletov (2009), The distribution of neodymium isotopes in Arctic Ocean basins, *Geochim. Cosmochim. Acta*, *73*, 2645–2659.

Rahmstorf, S. (2002), Ocean circulation and climate during the past 120,000 years, *Nature*, *419*, 207–214.

Rempfer, J., T. F. Stocker, F. Joos, J.-C. Dutay, and M. Siddall (2011), Modelling Nd-isotopes with a coarse resolution ocean circulation model: Sensitivities to model parameters and source/sink distributions, *Geochim. Cosmochim. Acta*, *75*, 5927–5950.

Reynolds, B. C., M. Frank, and R. K. O'Nions (1999), Nd- and Pb-isotope time series from Atlantic ferromanganese crusts: Implications for changes in provenance and paleocirculation over the last 8 Myr, *Earth Planet. Sci. Lett.*, *173*, 381–396.

Roberts, N. L., A. M. Piotrowski, J. F. McManus, and L. D. Keigwin (2010), Synchronous deglacial overturning and water mass source changes, *Science*, *327*, 75–78.

Roberts, N. L., A. M. Piotrowski, H. Elderfield, T. I. Eglinton, and M. W. Lomas (2012), Rare earth element association with foraminifera, *Geochim. Cosmochim. Acta*, *94*, 57–71.

Rudels, B., R. Meyer, E. Fahrbach, V. V. Ivanov, S. Østerhus, and D. Quadfasel (2000), Water mass distribution in Fram Strait and over the Yermak Plateau in summer 1997, *Ann. Geophys.*, *18*, 687–705.

Rudels, B., G. Björk, J. Nilsson, P. Winsor, I. Lake, and C. Nohr (2005), The interaction between waters from the Arctic Ocean and the Nordic Seas north of Fram Strait and along the East Greenland current: Results from the Arctic Ocean-02 Oden expedition, *J. Mar. Syst.*, *55*, 1–30.

Rutberg, R. L., S. R. Hemming, and S. L. Goldstein (2000), Reduced North Atlantic Deep Water flux to the glacial Southern Ocean inferred from neodymium isotope ratios, *Nature*, *405*, 935–938.

Sarnthein, M., et al. (1995), Variations in Atlantic surface ocean paleoceanography, 50°-80°N: A time-slice record of the last 30,000 years, *Paleoceanography*, *10*, 1063–1094, doi:10.1029/95PA01453.

Sarnthein, M., G. Bartoli, M. Prange, A. Schmittner, B. Schneider, M. Weinelt, N. Andersen, and D. Garbe-Schönberg (2009), Mid-Pliocene shifts in ocean overturning circulation and the onset of Quaternary-style climates, *Clim. Past*, *5*, 269–283.

Schaule, B. K., and C. C. Patterson (1981), Lead concentrations in the northeast Pacific: Evidence for global anthropogenic perturbations, *Earth Planet. Sci. Lett.*, *54*, 97–115.

Sharma, M., A. R. Basu, and G. V. Nesterenko (1992), Perspectives on the Arctic's shrinking sea-ice cove temporal Sr-, Nd- and Pb-isotopic variations in the Siberian flood basalts: Implications for the plume-source characteristics, *Earth Planet. Sci. Lett.*, *113*, 365–381.

Steiger, R. H., and E. Jäger (1977), Subcommission on geochronology: Convention on the use of decay constants in geo- and cosmochronology, *Earth Planet. Sci. Lett.*, *36*, 359–362.

Stein, R., and K. Fahl (2013), Biomarker proxy shows potential for studying the entire Quaternary Arctic sea ice history, *Org. Geochem.*, *55*, 98–102.

Tachikawa, K., C. Jeandel, and M. Roy-Barman (1999), A new approach to the Nd residence time in the ocean: The role of atmospheric inputs, *Earth Planet. Sci. Lett.*, *170*, 433–446.

Tachikawa, K., A. M. Piotrowski, and G. Bayon (2014), Neodymium associated with foraminiferal carbonate as a recorder of seawater isotopic signatures, *Quat. Sci. Rev.*, *88*, 1–13.

Tanaka, T., et al. (2000), JNdi-1: A neodymium isotopic reference in consistency with La Jolla neodymium, *Chem. Geol.*, *168*, 279–281.

Tütken, T., A. Eisenhauer, B. Wiegand, and B. T. Hansen (2002), Glacial-interglacial cycles in Sr and Nd isotopic composition of Arctic marine sediments triggered by the Svalbard/Barents Sea ice sheet, *Mar. Geol.*, *182*, 351–372.

von Blanckenburg, F., and T. F. Nägler (2001), Weathering versus circulation-controlled changes in radiogenic isotope tracer composition of the Labrador Sea and North Atlantic Deep Water, *Paleoceanography*, *16*, 424–434, doi:10.1029/2000PA000550.

Vorontsov, A. A., V. V. Yarmolyuk, G. S. Fedoseev, A. V. Nikiforov, and G. P. Sandimirova (2010), Isotopic and geochemical zoning of Devonian magmatism in the Altai–Sayan rift system: Composition and geodynamic nature of mantle sources, *Petrology*, *18*, 596–609.

Wahsner, M., C. Müller, R. Stein, G. Ivanov, M. Levitan, E. Shelekova, and G. Tarasov (1999), Clay-mineral distribution in surface sediments of the Eurasian Arctic Ocean and continental margin as indicator for source areas and transport pathways—A synthesis, *Boreas*, *28*, 215–233.

Werner, K., M. Frank, C. Teschner, J. Müller, and R. Spielhagen (2014), Neoglacial change in deep water exchange and increase of sea-ice transport through eastern Fram Strait: Evidence from radiogenic isotopes, *Quat. Sci. Rev.*, *92*, 190–207.

Wilson, D. J., A. M. Piotrowski, A. Galy, and I. N. McCave (2012), A boundary exchange influence on deglacial neodymium isotope records from the deep western Indian Ocean, *Earth Planet. Sci. Lett.*, *341*, 35–47.

Wilson, D. J., A. M. Piotrowski, A. Galy, and J. A. Clegg (2013), Reactivity of neodymium carriers in deep sea sediments: Implications for boundary exchange and paleoceanography, *Geochim. Cosmochim. Acta*, *109*, 197–221.

Wilson, D. J., A. Galy, A. M. Piotrowski, and V. K. Banakar (2015), Quaternary climate modulation of Pb isotopes in the deep Indian Ocean linked to the Himalayan chemical weathering, *Earth Planet. Sci. Lett.*, *424*, 256–268.

Winter, B., C. M. Johnson, and D. L. Clark (1997), Strontium, neodymium and lead isotope variations of authigenic silicate sediment components from the late Cenozoic Arctic Ocean: Implications for sediment provenance and the source of trace metals in sea water, *Geochim. Cosmochim. Acta*, *61*, 4181–4200.

Wolf, T. C. W., and J. Thiede (1991), History of terrigenous sedimentation during the past 10 m.y. in the North Atlantic (ODP Legs 104 and 105 and DSDP Leg 81), *Mar. Geol.*, *101*, 83–102.

Wolf-Welling, T. C. W., J. Thiede, A. M. Myhre, and Leg 151 Shipboard Scientific Party (1995), Bulk sediment parameter and coarse fraction analysis: Paleoceanographic implications of Fram Strait Sites 908 and 909, ODP Leg 151 (NAAG), *Eos Trans.*, *76*, Suppl., 166.

Zachos, J., M. Pagani, L. Sloan, E. Thomas, and K. Billups (2001), Trends, rhythms, and aberrations in global climate 65 Ma to present, *Science*, *292*, 686–693.